



## Joint ICTP-IAEA School on Data for Modelling Atomic and Molecular Processes in Plasmas | (SMR 3924)

18 Mar 2024 - 22 Mar 2024  
ICTP, Trieste, Italy

---

### P01 - AGRAWAL Ayushi

Diagnostics of Kr+ plasma using collisional radiative model with detailed electron impact fine-structure excitation cross-section calculations

### P02 - AJROUDI Imen

Precise relativistic calculation of atomic data for helium-like Iron (Fe<sup>24+</sup>): atomic structure and collision by electron impact

### P03 - ANSIA FERNÁNDEZ Lucas

Modelling non-thermal XFEL heating of solids

### P04 - ARIANTO Fajar

Diagnostics of plasma jet and dielectric barrier discharge plasma parameters by optical emission spectroscopy

### P05 - BABURAJ Geethika

Dynamics Of Polarized Emission From Nanosecond Laser-Produced Aluminum Plasma

### P06 - CHANDRA Ray

Lyman line opacities in tokamak divertor plasmas under high-recycling and detached conditions

### P07 - DANSER Xyoisan

The Bottom-Up Method: Measuring and controlling energy of tin ions \ emanating from laser produced plasmas

### P08 - DE LANGE Stan Johannes Jacobus

Simulations of plasmas driven by laser wavelengths in the 1.064 – 10.6 μm range as future extreme ultraviolet light sources

### P09 - DONOHOE Éanna John

Simultaneous Plasma Absorption Measurements from XUV to IR

### P10 - DOWD Kirsten Hollie

Near Infrared Photo-absorption in Plasmas for Astrophysical Applications

### P11 - DOYLE Eric

5p->nd, ms and 4f->nd EUV photoabsorption in Ir to Ir<sup>4+</sup>

### P12 - FAGAN Eoin Finn

EUV Photoabsorption Spectroscopy of Hf Laser Produced Plasmas

### P13 - GARBE Evan Francis

Improving Dielectronic Recombination Rate Coefficients for the Li- and Be-like Isoelectronic Sequences

### P14 - GHOSH Nitish

RELATIVISTIC CALCULATIONS OF ENERGY LEVEL, LIFETIMES, TRANSITION PARAMETERS, AND ELECTRON IMPACT EXCITATION CROSS SECTION FOR Xe<sup>36+</sup>

### P15 - GHOSH Raju

Bound and resonant states of the imidogen (NH) radical : An R-matrix study.

**P16 - JARDIN Axel Georges Rene**

Using X-ray measurements to assess uncertainties in plasma temperature and impurity profiles in tokamaks

**P17 - JIN Xuejian**

Study on the evolution of the plasma state of electric explosive wires

**P18 - KADI Lyes Roland**

Measurement of collisional-radiative matrix elements from the time evolution of laser-induced fluorescence

**P19 - KENNEY Zachary Adam**

Plasma Radiative properties experiments at AWE

**P20 - KOHLMEIER Felix Michael**

Measurement of EUV light in laser-produced plasma generated by a 2um laser on tin droplets

**P21 - KUMAR Ankit**

Edge Toroidal Rotation of Different Ions in ADITYA-U Tokamak

**P22 - MAISON Lucas Nathan S**

A new set of radiative decay rates for forbidden lines in lanthanide ions of interest for kilonova nebular phase studies

**P23 - MILDER Avram Lev**

Numerical investigation of ionization dynamics in intense laser-heated argon plasma using the NLTE model

**P24 - MONGEY Kevin Michael**

Soft x-ray emitting laser-produced plasmas: Advances in imaging, spectroscopy and simulation techniques

**P25 - MURRAY Kieran Augustine**

Poster on inferring the role of plasma-neutral interactions in tokamak divertors using hydrogen emission spectroscopy

**P26 - PARIKH Smruti Hareshkumar**

Electron interaction with Fluoromethanes

**P27 - PAULY Leya**

Enhancing Quantitative Analysis efficiency with Deep Learning Neural Network Coupled Laser-Induced Breakdown Spectroscopy

**P28 - SACKERS Marc Nicolas**

Unveiling the non-linear Zeeman effect in isotopes of krypton and xenon at the linear plasma device PSI-2

**P29 - SCHUTJES Kay**

Design of TALIF and CARS Diagnostics for Measuring Atomic and Molecular Hydrogen Densities in Divertor-relevant Plasmas

**P30 - SEKKAL HADDOUCHE Asma Farah**

Multipole rate coefficients for excitation of Fe XIII by isotropic Maxwellian electrons

**P31 - SHANMUGASUNDARAM Suriyaprasanth**

Electron and Positron impact partial ionization cross sections of diatomic molecules present in the interstellar medium

**P32 - SHIVANKAR**

Spectral properties of plasma embedded He-like Ar XVII under the influence of external magnetic field.

**P33 - SIDDIKI Mohammad Faisal Bin Touhid**

He / Ne Beam Line Ratio Spectroscopy to Investigate Plasma Boundary of Wendelstein 7-X Stellarator Fusion Experiment

**P34 - SINGH Gajendra**

Theoretical Investigation of anomalous Intensity Ratio of Spectral Lines of at 18.03 and 18.79 nm of Ar<sup>13+</sup> ion in ADITYA-U tokamak.

**P35 - SOHN Janghyeob**

Opacity calculations of various elements at a variety of plasma conditions using the improved FLYCHK code

**P36 - STAIGER Hunter William**

Diffraction Order Penalization to Improve Spectrometer Calibrations

**P37 - VARSHA SUNIL**

Development of Capacitively Coupled Radio Frequency Discharge Plasma Device for the Validation of Supersonic Molecular Beam Diagnostics using Collisional-Radiative Model.

**P38 - INDHU SURESH**

Fully relativistic calculation of cross sections and their application in identifying suitable emission lines for the diagnostics of non-equilibrium plasmas

**P39 - TIAN Ziqiang**

Hyperfine-induced effects on the linear polarization of the magnetic-quadrupole lines of spin-1/2 Be-like ions excited by electron impact

**P40 - WANG Baoguo**

Tomographic reconstructions of the 2D emission distributions of impurity with EAST visible tangential wide-angle viewing systems

**P41 - WANG Hui**

Comparative modeling of neon and tungsten impurity transport in the boundary plasma of EAST with normal and extended grid to the first wall

**P42 - WÜST Erik**

Deuterium retention analysis in pre-damaged tungsten using laser-induced breakdown spectroscopy

**P43 - WU Xiaoxia**

High energy density material produced by heavy ion beam drive

**P44 - YARON Peter Nikolaivich**

Charge exchange recombination spectroscopy of Ta<sup>q+</sup> for application to DIII-D and ITER neutral Hydrogen beam diagnostics

## Diagnostics of $\text{Kr}^+$ plasma using collisional radiative model with detailed electron impact fine-structure excitation cross-section calculations

Ayushi Agrawal<sup>1</sup>, Shivam Gupta<sup>2</sup>, Lalita Sharma<sup>1</sup> and Rajesh Srivastava<sup>1</sup>

<sup>1</sup>*Indian Institute of Technology Roorkee, India 247667*

<sup>2</sup>*National Institute for Fusion Science, Toki, Gifu 509-5202, Japan*

Low-pressure plasmas are having important applications such as in materials processing, in particular for deposition and etching of thin films for electronic, optoelectronic and photonic devices [1]. Recently, plasma of Kr and its ions have been explored and considered for such selected applications. In the present work, we consider the diagnostics of low-temperature  $\text{Kr}^+$  plasma using collisional radiative model (CR). We need extensive electron excitation cross-section data of the fine structure levels of  $\text{Kr}^+$  which are dominant process at low temperature. These cross-sections will be incorporated in the collisional radiative model. We applied the model to the optical emission spectroscopy measurements of  $\text{Kr}^+$ , reported by Mar et al.[2].

We have calculated electron impact excitation cross-sections of several levels of  $\text{Kr}^+$  using the fully relativistic distorted wave theory [3]. We determined the required wave functions of  $\text{Kr}^+$  in the multi-configuration Dirac-Fock approximation and validated them by comparing the calculated energy levels and some transition probabilities with previously reported values. In the CR model, some selected important excitation transitions from the ground, quasi-metastable and metastable states of  $\text{Kr}^+$  have been considered along with other plasma processes. We utilized the measured intensities of five emission lines of  $\text{Kr}^+$  [2] and compared these with the values obtained from the CR model to extract plasma parameters, specifically, the electron temperature, electron density and other plasma parameters.

[1] M A Lieberman and A J Lichtenberg, *Principles of Plasma Discharges and Materials Processing* (New York: Wiley) (2004).

[2] S Mar et al., *J. Phys. B: Atm, Mol. Opt. Phys.* **39** 3709, (2006).

[3] R Srivastava et al, *Phys. Rev. A.* **74**, 012715 (2006).

## Precise relativistic calculation of atomic data for helium-like Iron ( $Fe^{24+}$ ): atomic structure and collision by electron impact

Imen Ajroudi<sup>1</sup>, Dhia Elhak Salhi<sup>1</sup>, Soumaya Manai<sup>1</sup> and Haikel Jelassi<sup>1</sup>

<sup>1</sup>*Research laboratory on Energy and Matter for Nuclear Sciences Development, LR16CNSTN02, Tunisia. National Center for Nuclear Sciences and Technologies, Sidi Thabet Technopark 2020 Ariana Tunisia.*

We present a theoretical contribution to the study of the atomic structure and the collisional excitation process by electron impact (EIE) of the  $Fe^{+24}$  ion. This ion is selected regarding its capital interest in nuclear fusion. Our relativistic radiative and collisional properties have been calculated using Dirac-Fock-Slater (DFS) and Distreded waves (DW) both implemented in the FAC code. We started our study by calculating the lowest 71 energy levels belonging to the configuration  $1s^2$  and  $1snl$  with  $n$  varies from 1 up to 6. Breit and QED type corrections have been considered in our calculations. Our findings have been compared with NIST data and found to be in good agreement. Collisions strength values, for the first transitions between the ground level  $^1S_0$  and excited levels  $^3S_1$ ,  $^1S_0$ ,  $^3P_{0,1,2}$  and  $^1P_1$ , have been calculated and this for a series of incident energy between 0 and 20000 eV. We also carried out calculations of effective collision strengths and excitation rate for the same selected transitions, with chosen electronic temperature covering: 107.72, 268.86, 605.8, 1077.2, 1361.5, 2688.6 and 3033.3 eV. Our funding have been compared against those calculated by are made with other references and gives compatibility between the values compiled by Aggrawal et al [1] and Honglin Zhang et al [2].

[1] A.Kanti M Aggarwal a, B. Francis P Keenan. , Physica Scripta. **87(5):055302**, 1357 (app2013).

[2] A. Honglin Zhang , B. Douglas H. Sampson, Astrophysical Journal Supplement Series. **487–514**, 7531 (1987).

## Modelling non-thermal XFEL heating of solids

**Lucas Ansia<sup>1,2</sup>, Pedro Velarde<sup>2</sup>, Gareth Williams<sup>1</sup> and Marta Fajardo<sup>1</sup>.**

<sup>1</sup> *GoLP/Instituto de Plasmas e Fusão Nuclear-Laboratório Associado, Instituto Superior Técnico, Universidade de Lisboa, 1049-001 Lisboa, Portugal.*

<sup>2</sup> *Instituto de Fusión Nuclear, Universidad Politécnica de Madrid, José Gutiérrez Abascal 2, 28006 Madrid, Spain.*

Over the past two decades, X-ray free-electron lasers (XFELs) have made significant progress, achieving peak brightness in the XUV and X-ray regions that were previously only attainable in the optical and infrared ranges. This advancement has opened up new possibilities in high-energy density science. It enables the creation of solid-density plasmas with larger volumes, greater uniformity, and well-defined properties, including temperature and density.

To better comprehend experimental results, such as x-ray spectra, Collisional Radiative Models (CRM) have been extensively employed. This study focuses on simulating middle Z materials, specifically transition metals when subjected to XFEL irradiation. For this purpose, simulations have been carried out using BigBarT.

BigBarT is a CRM, already validated for the calculations of thermal opacities [1], that incorporates self-consistent treatment of the non-thermal effects in electronic distribution [2] together with degeneracy in the continuum electrons. These tools together will lead to a better understanding of collisional processes in extreme conditions relevant to inertial fusion and compact astrophysical objects.

[1] A. G. de la Varga, P. Velarde, *High Energy Density Physics* **7**, 163-168 (2011).

[2] A. G. de la Varga, P. Velarde, *High Energy Density Physics* **9**, 542-547 (2013).

## Diagnostics of plasma jet and dielectric barrier discharge plasma parameters by optical emission spectroscopy

**Fajar Arianto<sup>1</sup>, Eko Yulianto<sup>1</sup>, and Muhammad Nur<sup>1</sup>**

<sup>1</sup>*Center for Plasma Research, Department of Physics, Faculty of Science and Mathematics, Diponegoro University, Semarang, Central Java, Indonesia*

The plasma jet and dielectric barrier discharge plasma, non-thermal plasma type at atmospheric pressure, has drawn significant interest as a study subject across numerous scientific fields. Examples include material processing, nanotechnology, pollution control, atmospheric pressure plasma jets, surface modification of polymers for biological applications (medicine, healthcare, and plasma biology), and pollution control<sup>[1,2,3,4,5,6]</sup>. At gas flow rates between 1 and 5 liters per minute, this research abstract offers an experimental approach for determining the plasma properties in the jet plasma and dielectric barrier discharge plasma systems with molecular and atomic gas sources (Nitrogen, Oxygen, Argon, Helium and mixed gases) at varied voltage and standard atmospheric pressure<sup>[7]</sup>. This method is based on OES, or optical emission spectroscopy<sup>[8]</sup>. In emission spectroscopy, each spectral line represents an optical transition between the quantum states of two atoms or molecules. The concentrations of species in different higher stages determine the intensity of the spectral lines<sup>[8,9]</sup>. In low-pressure discharge systems, we calculated the electron density ( $n_e$ ) and electron temperature ( $T_e$ ) using ratios of line intensity and the Boltzmann equation<sup>[7]</sup>. Additionally, measurements were taken of the electron temperature and plasma properties linked to electron density, like ( $\lambda_D$ ,  $N_D$ , and  $\omega_p$ )<sup>[7,8,10]</sup>. The plasma was created using a variety of flow rates. The Debye length, plasma frequency, and particle number on the Debye surface are all strongly impacted by an increase in gas flow rate on the plasma characteristics, and they all rise with the gas flow rate.

### References:

- [1] Shouichiro Iio, Kosuke Yanagisawa, Chizuru Uchiyama, Katsuya Teshima, Naomichi Ezumi, Toshihiko Ikeda, *Surface & Coatings Technology* **206**, 1449–1453 (2011).
- [2] Sara Javanmard, Sohrab Gholamhosein Pouryoussefi, *Current Applied Physics* **46**, 61–69 (2023).
- [3] Muhammad Imran Nawaz, Chengwu Yi, Abdul Mannan Zafar, Rongjie Yi, Babar Abbas, Husseini Sulemana, Chundu Wu, *Environmental Research* **237**, 117015 (2023).
- [4] Yafei Zhai, Jiaqi Sun, Shuo Ye, Yuhao Wang, Jiali Tian, Yanhong Bai, Qisen Xiang, Ruiling Shen, *LWT - Food Science and Technology* **185**, 115089 (2023).
- [5] Zewei Wang, Qiannan Zhao, Yuan Gan, Qiuxia Fan, Zhongqiu Hu, Zhouli Wang, Rui Cai, Tianli Yue, Yahong Yuan, *Innovative Food Science and Emerging Technologies* **87**, 103415 (2023).
- [6] Jirarat Anuntagool, Natchanon Srangsomjit, Pimphak Thaweewong, Graciela Alvarez, *Food Control* **153**, 109913 (2023).
- [7] Harakat Mohsin Roomy a, N. Yasoob A., Hamid H. Murbat, *Kuwait Journal of Science* **50**, 163–167 (2023).
- [8] Himanshu Mishra, Milan Tichý, Pavel Kudrna, *Vacuum* **205**, 111413 (2022).
- [9] Yan-Fei Wang a, Xi-Ming Zhu, *Spectrochimica Acta Part B: Atomic Spectroscopy* **208**, 106777 (2023).
- [10] Nikolaos Giannakaris, Gustav Gürtler, Thomas Stehrer, Manuel Mair, Johannes D. Pedarnig, *Spectrochimica Acta Part B: Atomic Spectroscopy* **207**, 106736 (2023).

## Dynamics Of Polarized Emission From Nanosecond Laser-Produced Aluminum Plasma

**Geethika B R<sup>1,2</sup>, Jinto Thomas<sup>1,2</sup>, Milaan Patel<sup>1,2</sup>, Renjith Kumar R<sup>1,2</sup> and Hem Chandra Joshi<sup>1</sup>**

<sup>1</sup>*Institute For Plasma Research, Bhat, Gandhinagar, Gujarat, 382428, India*

<sup>2</sup>*Homi Bhabha National Institute, Training School Complex, Anushaktinagar, Mumbai, 400094, India*

Anisotropic emission from laser-generated plasma has been the focal point for improving the signal-to-noise ratio in laser-induced breakdown spectroscopy (LIBS). However, thorough understanding of the underlying physical mechanisms or atomic processes is not fully known. In addition, the spatio-temporal evolution of anisotropy in dynamic plasma such as laser plasma has not been systematically investigated. In this work, efforts are made to study the dynamic nature of the polarized emission at different spatial locations as well as times [1]. An attempt is being made to interpret the observed effects of polarization with the involved atomic and collisional processes.

Briefly, a pulsed Nd:YAG laser (10 ns) is used to generate plasma from an aluminium sample under a controlled background pressure of 100 mbar with ambient nitrogen. A polarization resolved imaging system coupled with a spectrometer and intensified charge coupled device (ICCD) is used to record the spectral emission features for both polarizations.

The spatial and temporal evolution of the degree of polarization (DOP) shows a dependence on the charge state and a sign reversal with distance from the sample for ionic emission. The observed behaviour of DOP close to the sample appears to be due to self-generated magnetic field. However, far from the sample, as the effect of this magnetic field is diminished, the observed DOP appears to result from the interaction of the plasma with background gas molecules.

We believe this study will provide further insights into the dynamics of polarized emission from laser-generated plasma, revealing novel phenomena with implications for the advancement in LIBS technology and understanding of plasma interactions.

- [1] B. R. Geethika, Jinto Thomas, Milaan Patel, Renjith Kumar R. and Hem Chandra Joshi, *J. Anal. At. Spectrom.* **38**, 2477 (2023).



## Lyman line opacities in tokamak divertor plasmas under high-recycling and detached conditions

R. Chandra<sup>1</sup>, D. Reiter<sup>2</sup>, N. Horsten<sup>3</sup>, M. Groth<sup>1</sup>

<sup>1</sup>*Aalto University, Department of Applied Physics, Espoo, Finland*

<sup>2</sup>*Institut for Laser and Plasmaphysics, Heinrich-Heine-Universität, Düsseldorf, Germany*

<sup>3</sup>*KU Leuven, Department of Mechanical Engineering, Leuven, Belgium*

The radiation transport modelling of deuterium Lyman series using EIRENE predicts a 20% enhancement of ionization in the JET-ILW low-confinement (L-mode) divertor plasma under high-recycling and detached conditions. Opacity of the hydrogen Lyman line radiation directly affects the population of electronically excited states and thereby affects the effective ionization rates and the spectroscopic interpretation of local plasma parameters [1, 2, 3]. Proper treatment of opacity requires a coupled solution between the collisional equilibrium of the involved species and radiation transport, both of which depends on the information of plasma temperature and density at all points in space. The opacity is calculated using an inline collisional-radiative model (CRM) [4] of the kinetic Monte Carlo model EIRENE [5, 6] from particle and photon trajectories. The CRM-EIRENE model is applied to plasma solutions provided by EDGE2D[7] and B2.5 (in SOLPS-ITER[8, 9]) fluid solvers for JET-ILW low confinement plasma with different separatrix densities representing low-recycling, high-recycling and detached conditions. In both boundary plasma code solutions, the model suggests high opacity of the Lyman- $\alpha$  and Lyman- $\beta$  lines in the JET divertor volume under high-recycling and detached plasma conditions.

This work has been carried out within the framework of the EUROfusion Consortium, funded by the European Union via the Euratom Research and Training Programme (Grant Agreement No 101052200 — EUROfusion). Views and opinions expressed are however those of the author(s) only and do not necessarily reflect those of the European Union or the European Commission. Neither the European Union nor the European Commission can be held responsible for them. This work has been supported by the Academy of Finland under grant no. 1330050. The results are obtained with the help of the EIRENE package (see [www.eirene.de](http://www.eirene.de)) including the related code, data and tools.

- [1] J. L. Terry et al., *Physics of Plasmas* **5** 1759–66 (1998)
- [2] S. Lisgo et al., *Journal of Nuclear Materials* **337–339** 139–45 (2005)
- [3] B Lomanowski et al., *Plasma Physics and Controlled Fusion* **62** 6:065006 (2020)
- [4] K. Sawada et al., *Journal of Applied Physics* **73** 8122 (1993)
- [5] D. Reiter et al., *Plasma Physics and Controlled Fusion* **44** 8:1723–37 (2002)
- [6] V. Kotov et al., *Contribution to Plasma Physics* **46** 635 – 642 (2006)
- [7] R. Simonini et al., *Contribution to Plasma Physics* **34** 368-373 (1994)
- [8] S. Wiesen et al., *Journal of Nuclear Materials* **463** 480–84 (2015)
- [9] X. Bonnin et al., *Plasma and Fusion Research* **11** 1403102–1403102 (2016)
- [10] N. Horsten et al., *Nuclear Materials and Energy* **33** 101247 (2022)

## The Bottom-Up Method: Measuring and controlling energy of tin ions emanating from laser produced plasmas

X. Danser BSc<sup>1</sup>, Y. Mostafa MSc<sup>1</sup>, and Prof. Dr. O.O. Versolato<sup>1</sup>

<sup>1</sup>(*Presenting author underlined*) *Advanced Research Center for Nanolithography*

Extreme ultraviolet lithography (EUVL) is essential for the mass production of the most advanced integrated circuits [1]. Laser produced plasmas (LPPs) are used for nanolithography because they are efficient sources of EUV light. The material of choice for EUVL is tin (Sn), because tin plasmas radiate in a tight band around 13.5 nm [2, 3]. This wavelength is important because there are no suitable lenses, which conventionally are used for lithography, for EUV light. To be able to image the nanolithography mask, multi-layer mirrors (MLMs) are used, Molybdenum-Silicon MLMs reflect 70% of light at  $13.5 \pm 0.135$  nm (so called 'in-band' light) [4]. However, not all of the energy of the input laser is converted to EUV radiation, debris are also created, to name a few: so called 'out of band' light, clusters of neutral atoms and tin ions are also created. The goal is to obtain a conversion efficiency (CE) that is as high as possible. Thus we would like to minimize the energy that goes into debris and maximize the energy that is converted to in-band light. Tin ions can be harmful debris, because they are able to damage the MLMs, deteriorating their reflection and reducing lifetime [3, 5]. Thus it is useful to obtain information about the kinetic energy that these ions have and to know under which angle they are ejected.

At the Advanced Research Center for Nanolithography (ARCNL) in Amsterdam, The Netherlands, fundamental research is done that is relevant for industrial nanolithography. My research is in the Extreme Ultraviolet (EUV) Plasma Processes group. My research focuses on tin ions emanating from laser produced plasmas in a setting comparable to industrial nanolithography. Using retarding field analysers (RFAs) and an analysis method developed at ARCNL, the Bottom-Up Method, we are able to get a charge resolved energy spectrum. Using 7 such RFAs allows us to also get an angularly resolved energy spectra, these show that emission is highly anisotropic. Currently my work is improving this method, identifying systematic effects that have not been included yet. In addition to this the aim is to see if it is possible to control the fraction of input energy that is converted to ion kinetic energy, by laser temporal or spatial shape for instance. My poster presentation will be about these systematic effects, and if possible will also include some results from experiments.

## References

- [1] D. J. Hemminga, O. Versolato, and J. Sheil, *Physics of Plasmas* **30**, 10.1063/5.0125936 (2023).
- [2] R. Schupp, F. Torretti, R. Meijer, M. Bayraktar, J. Sheil, J. Scheers, D. Kurilovich, A. Bayerle, A. A. Schafgans, M. Purvis, K. Eikema, S. Witte, W. Ubachs, R. Hoekstra, and O. Versolato, *Applied Physics Letters* **115**, 124101 (2019).
- [3] O. Versolato, *Plasma Sources Science and Technology* **28**, 083001 (2019).
- [4] D. J. Hemminga, L. Poirier, M. M. Basko, R. Hoekstra, W. Ubachs, O. Versolato, and J. Sheil, *Plasma Sources Science and Technology* **30**, 105006 (2021).
- [5] J. R. Freeman, S. S. Harilal, B. Verhoff, A. Hassanein, and B. Rice, *Plasma Sources Science and Technology* **21**, 055003 (2012).

## Simulations of plasmas driven by laser wavelengths in the 1.064 – 10.6 $\mu\text{m}$ range as future extreme ultraviolet light sources

**Stan J.J. de Lange,<sup>1,2</sup> Diko J. Hemminga,<sup>1,2</sup> Oscar O. Versolato,<sup>1,2</sup> and John Sheil<sup>1,2</sup>**

<sup>1</sup> *Advanced Research Center for Nanolithography,  
Science Park 106, 1098 XG Amsterdam, The Netherlands*

<sup>2</sup> *Department of Physics and Astronomy, and LaserLaB, Vrije Universiteit Amsterdam,  
De Boelelaan 1081, 1081 HV Amsterdam, The Netherlands*

We characterize the properties of extreme ultraviolet (EUV) light source plasmas driven by laser wavelengths in the  $\lambda_{\text{laser}} = 1.064 - 10.6 \mu\text{m}$  range and laser intensities of  $I_{\text{laser}} = 0.5 - 5 \times 10^{11} \text{ W cm}^{-2}$  for  $\lambda_{\text{laser}} = 1.064 \mu\text{m}$ . Detailed numerical simulations of laser-irradiated spherical tin microdroplet targets reveal a strong laser-wavelength dependence on laser absorptivity and the conversion efficiency of generating EUV radiation. For  $\lambda_{\text{laser}} = 1.064 \mu\text{m}$  irradiation, the increase in in-band radiation with increasing laser intensity is offset by only a minor reduction in conversion efficiency. Radiative losses are found to dominate the power balance for all laser wavelengths and intensities, and a clear shift from kinetic to in-band radiative losses with increasing laser wavelength is identified. Yet, with increasing laser intensity, such a shift is absent. We find that the existence of a maximum conversion efficiency, near  $\lambda_{\text{laser}} = 4 \mu\text{m}$ , originates from the interplay between the optical depths of the laser light and the in-band EUV photons for this specific droplet-target geometry.

## Simultaneous Plasma Absorption Measurements from XUV to IR

É. Donohoe<sup>1</sup>, E. Sokell<sup>1</sup> and F. O'Reilly<sup>1</sup>

<sup>1</sup>University College Dublin

*eanna.donohoe@ucdconnect.ie*

Here we present a proposed method of simultaneous absorption measurements in laser produced plasmas (LPPs) across a range of spectral regions from IR to XUV to rapidly acquire mutually corroborating sets of atomic data. The accurate interpretation of astrophysical spectra using atomic structure calculations and radiative transfer models requires as complete as possible a set of atomic data across a large spectral range. Particularly for the analysis of Kilonova spectra, elements of  $Z > 26$  which are thought to be formed via the r-process in binary neutron star mergers have very little atomic data available [1]. The UCD Atomic, Molecular & Plasma Physics group has done extensive work in the past in probing LPPs to measure relative absorbance [2, 3], particularly in the EUV region where ion populations can better be identified, and is currently working on IR and VUV photoabsorption experiments.

My PhD research is part of a broader effort funded through the IRC project GOIPG/2023/5067 and the ERC Synergy Award HEAVYMETAL. The focus of my work will be construction of an experiment which combines various probes and detectors to simultaneously take absorption measurements in multiple spectral regions. A soft x-ray probe, such as an LPP can be combined with a back illuminated CMOS to image the density profile of the plasma and measure uniformity. In tandem with this, a series of probes such as an OPO (600-2100nm) or Supercontinuum (400-2100nm) for VIS/IR or LPPs (<1nm – 400nm) for VIS/UV/EUV can be implemented with respective spectrometers and detectors to acquire absorption spectra. The experiment can be equipped with an ultrafast ICCD camera to acquire spectra with ps resolution, allowing the use of probes with temporal profiles longer than the plasma expansion time. Narrow band probes can also be used to image the spatial distribution of single ion stages. Combining all of these observation techniques allows extensive plasma diagnostics and the ability to obtain a large set of atomic data very rapidly.

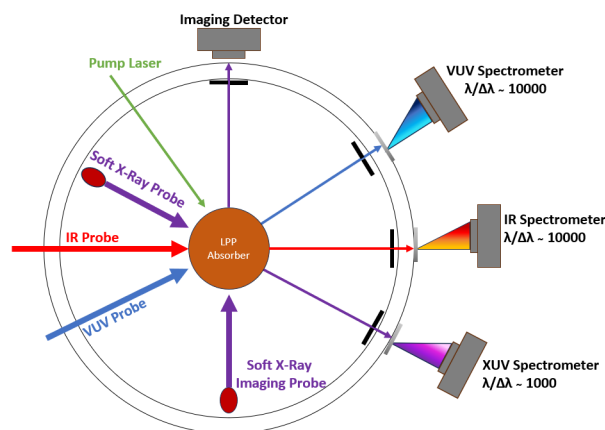


Figure 1: A probe-detector combination allowing absorption measurements in IR, UV & EUV simultaneously, with Soft X-Ray density imaging

- [1] J.H. Gillanders, M. McCann, S. Sim, S. Smartt, C. Ballance, Mon. Not. R. Astron. Soc. **506**, 3 (2021)
- [2] R. Stefanuik et al., Phys. Rev. A **101**, 3 (2020).
- [3] E. Doyle, G. O'Sullivan, P. Hayden, P. Dunne, J. Phys. B **56**, 13 (2023).

# Near Infrared Photo-absorption in Plasmas for Astrophysical Applications

Kirsten Dowd, Tom McCormack and Padraig Dunne

University College Dublin  
[kirsten.dowd@ucdconnect.ie](mailto:kirsten.dowd@ucdconnect.ie)

**Keywords:** NIR Absorption Spectroscopy, Laser Produced Plasma, Kilonova, AT2017gfo

This poster discusses the experimental design and results of the first iteration of near infrared (NIR) photo-absorption experiment. Half of the elements with  $Z > 26$  are believed to be synthesised via rapid neutron capture (r-process) in binary neutron star (BNS) mergers, due to their neutron rich and explosive environmental conditions [1]. Electromagnetic radiation is thermally emitted from the neutron rich ejecta of these events is mainly emitted in the ultraviolet (UV), optical and infrared spectral regions [2][3]. The first detection of such a kilonova event occurred in August 2017. Photometric and spectroscopic follow up observations were carried out to observe the evolution of this event. To accurately model merger events and identify elements synthesised in the AT2017gfo kilonova spectra, precise experimental values of wavelengths, oscillator strengths and atomic cross sections for absorption lines present in a wide range of heavy elements are required. Currently, a set of complete atomic data for elements present in the visible and NIR spectra of AT2017gfo, and those theorised to be formed in BNS mergers does not exist [4].

This project aims to develop a new NIR photo-absorption experiment using laser produced plasmas (LPP) to obtain a more complete set of experimentally found NIR atomic line lists. The experimental set up currently consists of a tuneable, broadband optical parametric oscillator (OPO), a neodymium-doped yttrium aluminium garnet (Nd: YAG) and an Acton SpectraPro 2750 Czerny-Turner Spectrometer. The Nd: YAG laser acts as the pump, generating the absorbing plasma while the OPO is used as the continuum source probe. The experimental setup is shown in Figure 1. The Nd: YAG is fired first and is incident on a metal target, generating a LPP. The OPO laser is fired after a set time delay,  $\Delta t$ , and is absorbed by the target plasma. The I and  $I_0$  laser beams are incident on different regions of the spectrometer slit. The time delay is varied in order to probe different ion stages present in the plasma. Using this experimental set up, absorption lines of four elements have been found, yttrium, zirconium, niobium and vanadium, in narrow bands of the NIR between 870 and 930 nm.

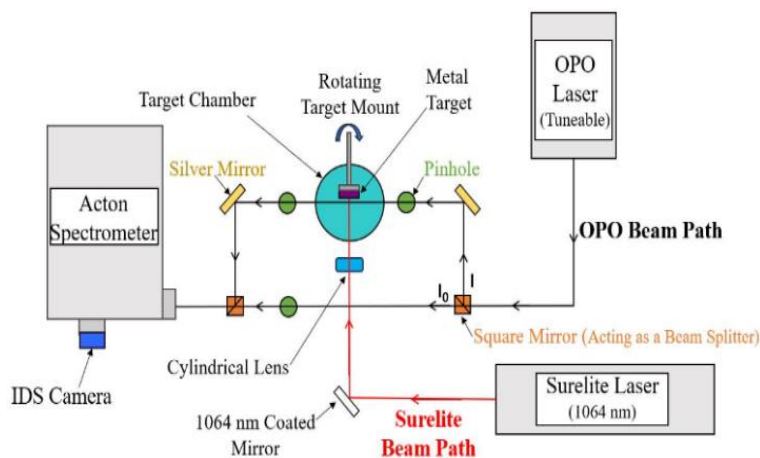


**Fig 1:** Diagram showing the NIR photo-absorption experimental apparatus.

## References

- [1] Watson et al., *Nature*, 574(7779), pp.497-500 (2019).
- [2] Smartt et al., *Nature*, 551(7678), pp.75-79 (2017).
- [3] Kasen et al., *Nature*, 551(7678), pp.80-84 (2017).
- [4] Gillanders et al. 2021. *Monthly Notices of the Royal Astronomical Society*, 506(3), pp.3560-3577 (2021).

## 5p → nd, ms and 4f → nd EUV photoabsorption in Ir to Ir<sup>4+</sup>

E. Doyle, E. Fagan, P. Hayden, and P. Dunne

*UCD School of Physics, University College Dublin, D04 P7W1, Dublin 4, Ireland*

Laboratory-based photoabsorption data are used to facilitate the identification of atomic transitions in astronomical rapid neutron-capture process (r-process) measurements [1]. Iridium is one of the elements in the third peak of the nucleosynthetic r-process, but very little knowledge is currently available for the inner-shell atomic structure of Ir ions [2].

Photoionization cross-section measurements of neutral Ir between 50-400 eV were recorded by direct photoabsorption of synchrotron radiation [3]. Subsequently, three lines due to Ir absorption and one line due to Ir<sup>+</sup> were detected by the Space Telescope Imaging Spectrograph which is aboard the Hubble Space Telescope [4].

Photoabsorption transition arrays arising from Ir to Ir<sup>4+</sup> ions have been recorded between 48-100 eV using the dual-laser plasma (DLP) technique [5], and were identified with the assistance of atomic structure calculations processed by the Cowan suite of atomic codes [6].

The theoretical absorption cross-section was determined by fitting each of the simulated electronic transitions with a Lorentzian profile [7], weighed by the Boltzmann population energy distribution for an electron temperature estimated by a collisional radiative model [8, 9], and convolved using a Gaussian of 0.05 eV linewidth to account for instrumental broadening.

The inner-shell spectra of laser-produced plasmas (LPPs) [10], which depend on initial laser and target conditions, will allow characterisation of the spatial and temporal evolution of the absorbing plasma. This determination will support the use of LPPs as sources of ions for spectroscopy in the UV, visible, and NIR regions of the spectrum, and will contribute to the interpretation of kilonova spectra in the future.

- [1] J. J. Cowan, C. Sneden, J. E. Lawler, A. Aprahamian, M. Wiescher, K. Langanke, G. Martínez-Pinedo, and F. K. Thieleman, *Rev. Mod. Phys.* **93**, 015002 (2021).
- [2] Kramida, Yu. Ralchenko, J. Reader, NIST ASD Team, NIST Atomic Spectra Database **5.11**, (2023).
- [3] M. Cukier, P. Dhez, P. Jaeglé, and F. C. Farnoux, *Phys. Lett. A* **51**, 173–4 (1975).
- [4] I. U. Roederer and J. E. Lawler, *Astrophys. J.* **750**, 76 (2012).
- [5] L. Gaynor, N. Murphy, P. Dunne, G. O’Sullivan, *J. Phys. B: At. Mol. Opt. Phys.* **41**, 245002 (2008).
- [6] A. Kramida, *Atoms* **7**, **64**, (2019).
- [7] E. Doyle, G. O’Sullivan, P. Hayden, P. Dunne, *J. Phys. B: At. Mol. Opt. Phys.* **56**, 135002 (2023).
- [8] D. Colombant and G. F. Tonon, *J. Appl. Phys.* **44**, 3524–37 (1973).
- [9] N. L. Wong, F. O’Reilly, E. Sokell, *Atoms* **8**, **56**, (2020).
- [10] P. K. Carroll and E. T. Kennedy, *Contemp. Phys.* **22**, 61-96 (1981).

**This research was supported by the Irish Research Council under grant GOIPG/2018/2827 and Horizons Europe under grant 101071865 HEAVYMETAL.**

## EUV Photoabsorption Spectroscopy of Hf Laser Produced Plasmas

E. Fagan, E. Doyle, F. O'Reilly, P. Dunne

*UCD School of Physics, University College Dublin, D04 P7W1, Dublin 4, Ireland*

Very little atomic structure information is documented for the lower ionisation stages of 6th row elements above 30 eV [1]. Spectroscopic studies of hafnium (Hf) emission have been carried out in previous focused campaigns [2, 3] as well as studies of the isoelectronic series of ion transitions across hafnium, tantalum, rhenium & tungsten [4, 5].

Lowly ionised hafnium photoabsorption spectra in the 47-160 eV region were recorded using the dual-laser plasma technique [6], utilising tungsten as a back-light continuum source to probe a line plasma generated by focussing 1064 nm Nd:YAG radiation through a cylindrical lens onto a hafnium target. These spectra were recorded on a  $\frac{1}{4}$  metre, flat field grazing incidence spectrometer, with a 1200 g/mm grating and a 2048 x 2048 pixel CCD camera, with inter-plasma time delays varied between 0-500 ns using a digital delay generator. A series of motors with micron accuracy were used to vary the x, y and z position of the targets and lenses, inside a vacuum chamber held at a pressure of  $10^{-4} - 10^{-5}$  mbar. Varying the position of the absorber target with respect to the optical axis allowed different regions of the absorber plasma to be probed. Varying the position of the absorber lens with respect to the absorber target modified the focussing conditions of the absorber plasma. This allowed variation of the laser power density in order to optimise conditions for the distribution of particular ion stages within the absorber plasma. The absorbance,  $A$ , was determined using Eq. 1 [7]:

$$A = \log_{10} \left( \frac{I_0}{I} \right) \quad (1)$$

Here  $I_0$  refers to the continuum radiation captured from the tungsten back-light plasma, and  $I$  refers to that continuum captured after passing through an absorbing Hf plasma. Calculations are underway using the Cowan Suite of Atomic Codes [8] for Hf I-VI ions to begin the process of line identification in the photoabsorption spectra. FLYCHK [9] and a modified version of a simple, single temperature collisional radiative model [10] will be utilised in combination with line identification to estimate the electron temperature at different inter-plasma time delays for generation of synthetic spectra. Work completed to characterise these Hf plasmas in the extreme ultraviolet (EUV) will form the basis of future work in analysis of EUV absorption in plasmas for Hf other 6th row elements which will assist in ion identification for the characterisation & line identification of near infrared plasmas.

- [1] A. Kramida, Yu. Ralchenko, J. Reader, NIST ASD Team, NIST Atomic Spectra Database **5.11** (2023).
- [2] J. Sugar, V. Kaufman, J. Op. Soc. America **64**, 1656 (1974).
- [3] P. Klinkenberg, T. Van Kleef, P. Noorman, Physica **27**, 1177 (1961).
- [4] A. N. Ryabtsev, E. Ya. Kononov, R. R. Kildiyarova, W. Ü. Tchang-Brillet, J. F. Wyart, Optics and Spectroscopy **112**, 109 (2012).
- [5] A. N. Ryabtsev, E. Ya. Kononov, R. R. Kildiyarova, W. Ü. Tchang-Brillet, J. F. Wyart, N. Champion, C. Blaess, Phys. Scr. **89**, 115402 (2014).
- [6] L. Gaynor, N. Murphy, P. Dunne, G. O'Sullivan, J. Phys. B: At. Mol. Opt. Phys. **41**, 245002 (2008).
- [7] E. Doyle, G. O'Sullivan, P. Hayden, P. Dunne, J. Phys. B: At. Mol. Opt. Phys. **56**, 135002 (2023).
- [8] A. Kramida, Atoms **7**, 64 (2019).
- [9] H. K. Chung, M. H. Chen, W. L. Morgan, Yu. Ralchenko, R. W. Lee, High Energy Density Physics **1**, 3 (2005).
- [10] N. L. Wong, F. O'Reilly, E. Sokell, Atoms **8**, 56 (2020).

## Improving Dielectronic Recombination Rate Coefficients for the Li- and Be-like Isoelectronic Sequences

**Evan Garbe<sup>1</sup>, Zahra Taghadomi Sarabi<sup>1</sup>, Phillip Stancil<sup>1</sup>, Isaac Garcia<sup>2</sup>, Stuart Loch<sup>2</sup>, Michael Fogle<sup>2</sup>, Nicholas Sterling<sup>3</sup>**

*<sup>1</sup>University of Georgia, <sup>2</sup>Auburn University, <sup>3</sup>University of West Georgia*

The ionization balance in a collisionally-ionized plasma is controlled primarily by a competition between electron-impact ionization and electron recombination processes. Of these, the rate coefficients for dielectronic recombination (DR) are the most difficult to calculate or measure and therefore contribute the primary driver of uncertainty in ionization balance of low temperature astrophysical plasmas. Focusing on the beryllium and lithium isoelectronic sequences, we will present new calculated rates using the public-domain package AUTOSTRUCTURE. As DR is sensitive to the location of near-threshold doubly-excited states in the continuum, we explore a range of methods beyond the usually adopted Hartree-Fock and Thomas-Fermi-Dirac-Amaldi central field approximations and compare to available experimental data. We also explore the effect of variations in the DR rate coefficients to the ionization balance in benchmark planetary nebula models with the astrophysical plasma package Cloudy. This work is partially supported by NSF grants AST-2108649 and NASA grant NASA-80NSSC21K1465.

- [1] N. Badnell, <http://http://amdpp.phys.strath.ac.uk/tamoc/DATA/DR/> (2011)
- [2] S. Böhm et al. A&A 405 3, 1157-1162 (2003)
- [3] S. Böhm et al. A&A 437 3, 1151-1157 (2005)
- [4] J. Colgan et al. A&A 417 3, 1183-1188 (2004)
- [5] J. Colgan et al. A&A 412 2 597-601 (2003)
- [6] G. J. Ferland et al. The 2017 Release Cloudy version 17.03 A&A 53, 385-438 (2017)
- [7] M. Fogle et al. A&A 442 2, 757-766 (2005)
- [8] A. Müller, Advances in Atomic Molecular and Optical Physics, 55, 293-417 (2008)
- [9] I. Orban et al. A&A 489, 829 (2008)
- [10] I. Orban et al. The Astrophysical Journal, 721 (2010)
- [11] S. Schippers et al. The Astrophysical Journal, 555, 1027 (2002)
- [12] S. Schippers et al. A&A 1 (2004)



# RELATIVISTIC CALCULATIONS OF ENERGY LEVEL, LIFETIMES, TRANSITION PARAMETERS, AND ELECTRON IMPACT EXCITATION CROSS SECTION FOR Xe<sup>36+</sup>

**Nitish Ghosh<sup>1</sup>, Lalita Sharma<sup>1</sup>**

<sup>1</sup>(Nitish Ghosh) Indian institute of technology Roorkee, Roorkee-247667

Atomic structure parameters for inert gas ions are in great demand due to their applications in fusion plasma modeling and diagnostics. In fusion devices, various charge states of inert gases ions can exist. Thus, it is of prime importance to have their reliable atomic data to assist in various ongoing projects on the design and development of fusion reactors. From the literature we found that there are very limited experimental or theoretical works available for atomic parameters of Xe<sup>36+</sup>. In this connection, we calculated energies, lifetimes, transition rates of the lowest 128 levels of Xe<sup>36+</sup> using multi-configuration Dirac-Hartree-Fock (MCDHF) method and many body perturbation theory (MBPT). The levels considered arise from 3s<sup>2</sup>3p<sup>6</sup>, 3s<sup>2</sup>3p<sup>5</sup>3d, 3s3p<sup>6</sup>3d, and 3s<sup>2</sup>3p<sup>4</sup>3d<sup>2</sup> configurations. The MCDHF results are obtained using the GRASP2018 [1] code, whereas flexible atomic code (FAC) [2] is employed to compute MBPT results. Breit interaction and quantum electrodynamics (QED) effects which are important for highly charged ions, are also accounted for in the present computations. Furthermore, using the relativistic distorted wave theory as described in reference [3], we have calculated electron impact excitation cross section of all transitions to upper levels from the ground and metastable levels for the incident electron energies up to 10 keV. We also provided analytical fittings of these cross sections for their applications in plasma modeling.

[1] **C. F. Fischer**, G.Gaigalas, G., Jönsson, J. Bieroń., *Computer Physics Communications*, Volume No. 237, Pages No. 184-178 (2019).

[2] **M. F. Gu**, *Canadian Journal of Physics*, Volume No. 86, Pages No. 675-689 (2008).

[3] **L.Sharma**, A.Surzhykov, R.Srivastava, S. Fritzsche, *Physical Review A*, Volume No. 83, Pages No. 062701 (2011).

R. Ghosh,<sup>1,\*</sup> K. Chakrabarti,<sup>2</sup> and B. S. Choudhury<sup>1</sup><sup>1</sup>Department of Mathematics, Indian Institute of Engineering Science and Technology, Shibpur, Howrah 711103, India<sup>2</sup>Department of Mathematics, Scottish Church College, 1 & 3 Urquhart Sq., Kolkata 700006, India

The NH imidogen radical is a common component in nitrogen chemical reactions that take place in the atmosphere and interstellar medium (ISM). Its existence was first observed in the 1990s in diffuse clouds [1], although it had been previously identified in the sun's atmosphere [2], stellar atmospheres and comet tails [3]. NH is also likely to be present and is a precursor to ammonia formation in the ISM [4].

NH and NH<sup>+</sup> are also produced during the combustion of nitramine compounds in rocket propellants, explosives, and emergency escape devices. Many nitrogen plasmas contain NH<sup>+</sup> and NH, therefore, the dynamics calculations and kinetic modeling of these products require electronic structure data and collision data in the form of potential energy curves, reaction rate coefficients and cross-sections [5].

Using the R-matrix method, low-energy electron collision calculations have been performed on NH<sup>+</sup> at its equilibrium geometry after building a suitable model to represent the target ion [6]. Scattering calculations are performed to obtain NH bound states for <sup>3</sup>Σ<sup>-</sup>, <sup>3</sup>Π, <sup>3</sup>Σ<sup>+</sup>, <sup>1</sup>Π, <sup>1</sup>Δ, <sup>1</sup>Σ<sup>-</sup>, <sup>1</sup>Σ<sup>+</sup>, <sup>5</sup>Σ<sup>-</sup>, <sup>5</sup>Π symmetric and resonance parameters for <sup>1</sup>Σ<sup>-</sup>, <sup>1</sup>Π and <sup>3</sup>Π symmetric as a function of geometry ranging from 1-9 a<sub>0</sub> on a moderately dense grid of 61 points. To illustrate the relative position of the low-lying states, we present the potential energy curves (PECs) of the ground state and the eight lowest excited states of NH in figure 1. We also compare our ground state with the work of Owono *et al* [7]. It is clear that there is a good agreement. Numerous resonances are characterised by the characteristic oscillations in the eigenphase sums of <sup>1</sup>Σ<sup>-</sup>, <sup>1</sup>Π and <sup>3</sup>Π overall symmetric of the e+ NH<sup>+</sup> system. It has been observed that many resonances occur in a series characterized by their effective quantum numbers  $\nu$  [6]. Many of these resonances have very narrow widths and may be close to crossing an NH<sup>+</sup> ion curve from above. To obtain an accurate representation, we are processing a detailed construction of the potential energy curves for the ion NH<sup>+</sup> and resonant states as the inter-nuclear distance R varies. Other collisional calculations should benefit from these resonant states, particularly the Dissociative Recombination of the NH<sup>+</sup> ion.

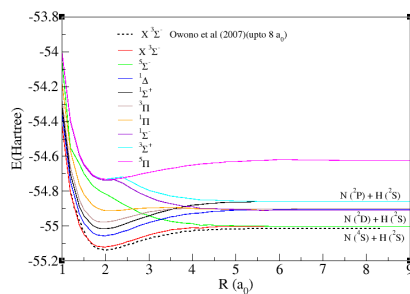


FIG. 1. Potential energy curves of the ground and eight lowest bound states of NH.

- [1] D. M. Meyer and K. C. Roth, *Astrophys. J. Lett.* **376**, L49 (1991).  
 [2] H. D. Babcock, *Astrophys. J.* **102**, 154 (1945).  
 [3] R. Meier, D. Wellnitz, S. J. Kim, and M. F. A'Hearn, *Icarus* **136**, 268 (1998).  
 [4] E. T. Galloway and E. Herbst, *Astron. Astrophys.* **211**,

- 413 (1989).  
 [5] G. F. Adams and R. W. Shaw, Jr., *Annu. Rev. Phys. Chem.* **43**, 311 (1992).  
 [6] R. Ghosh, K. Chakrabarti, and B. S. Choudhury, *Plasma Sources Sci. Technol.* **31**, 065005 (2022).  
 [7] L. C. O. Owono, N. Jaidane, M. G. K. Njock, and Z. B. Lakhdar, *J. Chem. Phys.* **126**, 244302 (2007).

\* rajughosh152@gmail.com

## Using X-ray measurements to assess uncertainties in plasma temperature and impurity profiles in tokamaks

A. Jardin<sup>1</sup>, J. Bielecki<sup>1</sup>, D. Dworak<sup>1</sup>, D. Guibert<sup>2</sup>, K. Król<sup>1</sup>, D. Mazon<sup>2</sup>, Y. Savoye-Peysson<sup>2</sup>, M. Scholz<sup>1</sup> and J. Walkowiak<sup>1</sup>

<sup>1</sup> *Institute of Nuclear Physics Polish Academy of Sciences (IFJ PAN), PL-31-342, Krakow, Poland.*

<sup>2</sup> *CEA, IRFM, F-13108 Saint-Paul-lez-Durance, France.*

In tokamaks, the local X-ray plasma emissivity is a complex quantity resulting from the contribution of several plasma parameters, i.e. electron temperature, density and concentration of impurities in multiple ionization states. In particular, the impurity core concentration can be estimated from the emissivity in the soft X-ray (SXR) range 0.1 – 20 keV, while information about the superthermal electron population can be obtained in the hard X-ray (HXR) range 20 keV – 200 keV [1]. The estimation of the tungsten concentration profile is subject to many uncertainties, in particular it requires accurate knowledge of plasma temperature, magnetic equilibrium, atomic processes leading to its cooling factor and the spectral response of the diagnostic [2]. A global W concentration can, for example, be inferred with integrated simulation codes in order to match the total radiated power. When all other plasma parameters are well-known, the impurity density profile can be reconstructed in the core with the help of SXR tomographic tools [3]. Nevertheless, in the case of a significant fraction of superthermal electrons e.g. due to RF heating, accurate estimation of electron temperature from ECE measurements can become a challenging task [4].

Therefore, the goal of this contribution is to establish a methodology to assess the uncertainty in the core electron temperature and impurity concentration profiles based on X-ray measurements. The proposed strategy is to define a grid of candidates ( $T_e$ ,  $c_w$ ) scenarios and identify the ones having the highest consistency with respect to multiple line-integrated measurements. In order to determine the capabilities and limitations of such an approach, the method is first tested on well-known synthetic profiles in an arbitrary tokamak geometry. In a second step, first experimental tests are presented for some selected WEST discharges.

[1] D. Mazon, et al (2022) JINST 17 C01073.

[2] T. Pütterich et al (2010) Nucl. Fusion 50 025012.

[3] A. Jardin et al (2021) Eur. Phys. J. Plus 136:706.

[4] P. V. Subhash et al (2017) Fusion Sci. Technol. 72 49–59.

**Acknowledgements.** *This work has been partially funded by the National Science Centre, Poland (NCN) grant HARMONIA 10 no. 2018/30/M/ST2/00799. We gratefully acknowledge Poland's high-performance computing infrastructure PLGrid (HPC Centers: ACK Cyfronet AGH) for providing computer facilities and support within computational grant no. PLG/2022/015994. This work has been carried out within the framework of the EUROfusion Consortium, funded by the European Union via the Euratom Research and Training Programme (Grant Agreement No 101052200 — EUROfusion). Views and opinions expressed are however those of the authors only and do not necessarily reflect those of the European Union or the European Commission. Neither the European Union nor the European Commission can be held responsible for them. This project is co-financed by the Polish Ministry of Education and Science in the framework of the International Co-financed Projects (PMW) programme Contract No 5450/HEU - EURATOM/2023/2.*

## Study on the evolution of the plasma state of electric explosive wires

**Xuejian Jin**<sup>1,2</sup>, **Rui Cheng**<sup>1,2</sup>, **Xinwen Ma**<sup>1,2</sup>, **Xiaoxia Wu**<sup>1,2</sup>

<sup>1</sup> *University of Chinese Academy of Sciences, Beijing 100049, China*

<sup>2</sup> *Institute of Modern Physics, Chinese Academy of Sciences, Lanzhou 730000, China*

Warm dense matter (WDM) is one of the core research topics in astrophysics, inertial confinement fusion, and high-energy density physics. Generally, WDM has a density ranging from 0.001 to 10 times the normal density and a temperature ranging from 0.1 to 100 eV. There are many ways to generate warm dense matter in the laboratory. The plasma generated by the exploding wire technique is initially in the WDM range after the wire explosion. The plasma has the advantages of axial symmetry and uniformity along the wire direction, which gives it certain advantages in plasma state diagnosis and characteristic studies. Moreover, the plasma state in the later stage has a relatively long lifetime (several  $\mu\text{s}$ ) and is relatively stable, making it suitable for related research as a relatively low-density plasma target<sup>[1-2]</sup>.

We have designed and constructed an exploding wire plasma discharge device and performed corresponding discharge experiments and diagnostic tests in air : Capacitor 4  $\mu\text{F}$  ; High voltage 10 kV; The wire 0.2 mm copper. The plasma was photographed using an ICCD camera, and the multiple repeated photographs showed excellent repeatability and stability of the discharge. Therefore, the discharge process can be described by photographing at different time points in multiple experiments, as shown in the figure 1. At the same time, we used multiple photodetectors of different wavelengths to diagnose its spontaneous emission and used the gray body radiation approximation to calculate the plasma temperature, obtaining a temperature variation of 0.5 to 1 eV in the first 200 ns after ignition. Due to time constraints, density measurement using laser interferometry has not been performed. However, based on volume expansion estimation, the average density is above 0.005 times the normal density, which can be considered close to the WDM state.

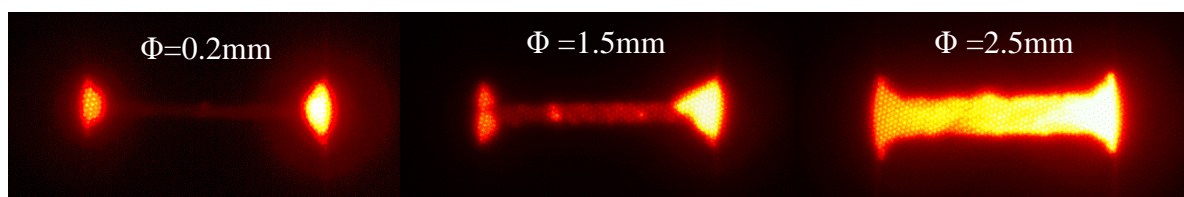


Figure 1. ICCD image: a)  $t=0$ ,  $\Phi=0.2\text{mm}$ ; b)  $t=100\text{ns}$ ,  $\Phi=1.5\text{mm}$ ; c)  $t=200\text{ns}$ ,  $\Phi=2.5\text{mm}$

The laser interferometry can provide density evolution for plasmas with densities below  $10^{20}\text{cm}^{-3}$ . Spectrometers and other devices can capture the evolution of spontaneous emission spectra. However, information such as ion charge state and opacity in the plasma cannot be directly obtained. Therefore, it is necessary to use other methods, such as simulation programs combined with temperature and density data, to calculate and obtain new plasma evolution information and verify the accuracy of the simulation program using spectroscopic data. Currently, we are studying the use of FAC and FLYCHK simulation programs, and the simulation results can also verify the applicability of the relevant programs in exploding wire plasma.

[1] Braams C M . Gastroenterology, 2002, 44(8):1767.

[2] Sarkisov G S, et al.. Physical Review E, 2005, 71(4): 046404.

## Measurement of collisional-radiative matrix elements from the time evolution of laser-induced fluorescence

**L. Kadi<sup>1</sup>, C. Stollberg<sup>1</sup>, M. Baquero-Ruiz<sup>1</sup>, and I. Furno<sup>1</sup>**

<sup>1</sup> *Ecole Polytechnique Fédérale de Lausanne (EPFL), Swiss Plasma Center (SPC), CH-1015 Lausanne, Switzerland*

Laser-induced fluorescence (LIF) is a widely used diagnostic tool in the study of low-temperature plasmas. LIF experiments usually focus on analysing the signal in the spectral domain, which allows the determination of the velocity distribution function (VDF) of the probed species. From the VDF several key parameters can be extracted, such as the temperature and flow velocity, as well as the density if an absolute calibration is performed. The temporal behaviour of the LIF signal is more difficult to study owing to the fact that its accurate determination requires ultrashort laser pulses ( $\ll 1$  ns) and a high temporal resolution ( $\leq 1$  ns) of the detection system. LIF with ultrashort laser pulses effectively allows an instantaneous perturbation of the densities of the absorbing and laser-pumped states. The time evolution of the density of an excited state after absorption of the pulse is determined by reaction rates that populate or depopulate the state and is described by the rate equation  $\frac{d\vec{n}}{dt} = M\vec{n}$ . By pumping a state  $i$  and measuring the temporal evolution of the fluorescence emitted by a state  $j$ , it may be possible to determine the total reaction rate from  $i$  to  $j$  and therefore the matrix element  $M_{ij}$  [1].

As an example of this approach, we present time-resolved measurements of the fluorescence signal performed using the recently installed two-photon absorption laser-induced fluorescence (TALIF) diagnostic on the RAID linear device [2,3]. A ps laser system tuned to 205.1 nm is used to excite ground state H atoms into the  $n=3$  states. The subsequent decay of the  $n=3$  states is monitored at high temporal resolution ( $< 3$  ns) by recording the intensity of the Balmer alpha line (656 nm) using a fast-gated ICCD camera. The time evolution of the fluorescence signal is close to exponential, with an e-fold time  $\leq 10$  ns, corresponding to the inverse of the total depopulation rate of the  $n=3$  state [4] and the matrix element  $M_{33}$ .

This work was partially supported by the Swiss National Fund grant No 200020\_204983.

- [1] R. Denkelmann et al. J. Phys. B: At. Mol. Opt. Phys. 32 4635 (1999)
- [2] I. Furno, et al., EPJ Web of Conferences 157, 03014 (2017).
- [3] R. Jacquier et al., Fusion Engineering and Design 192 113614 (2023).
- [4] M.G.H. Boogaarts et al., Rev. Sci. Instrum., Vol. 73 (2002).

## Plasma Radiative properties experiments at AWE

Zachary Kenney AWE and D.J. Hoarty AWE

X-ray spectra are pivotal in the diagnosis of plasma properties experiments. Of a particular interest in the high temperature plasma physics experiments at AWE is the diagnosis of the plasma temperature and density inferred from the K-shell emission line ratios, for example the  $\text{He}_{\beta}/\text{Ly}_{\beta}$  line ratios, and the Stark Broadening by modelling the sample material's X-ray emission spectrum [1]. Recently, K shell X-ray absorption spectra of low Z elements have been obtained from short pulse laser heated experiments conducted at the ORION high power laser at AWE [2,3,4]. We present the experimental K-shell absorption spectra obtained from such experiments using a potassium chloride (KCl) sample, as part of an experimental platform development for short pulse heated hot, dense absorption experiments [1]. AWE's Orion laser uses short pulses to induce resistive heating in multilayer foil targets. A transverse temperature gradient in the heating is exploited to produce a hot, dense gold layer that acts to backlight the KCl sample heated up to temperatures in excess of 300eV, at near solid density [1]. Theoretical models of both CH (assumed to be pure C) and KCl were used to generate synthetic spectra to compare to the KCl measurements [4]. Due to the high temperature of the KCl sample, assumption of local thermodynamic equilibrium (LTE) was investigated by using non-LTE models. AWE's average atom opacity code, CASSANDRA, was used to generate spectra assuming an LTE model and the atomic kinetics code, FLYCHK, was executed to generate a non-LTE model spectrum of KCl [5,6,7]. The KCl modelling accounted for possible gradients in the sample by combining model spectra at different temperatures.

- [1] D.J Hoarty AWE, Private Communication (2023).
- [2] D. J Hoarty et al, Modelling K shell spectra from short pulse heated buried microdot targets, High Energy Density Physics, Volume 23, Pages 178-183, ISSN 1574-1818 (2017).
- [3] D. Hiller et al., Appl. Opt. 52, 4258-4263 (2013).
- [4] D. J. Hoarty et al. Observations of the Effect of Ionization-Potential Depression in Hot Dense Plasma. Phys. Rev. Lett. 110, 265003 (2013).
- [5] D.J. Hoarty et al, Measurements of emission spectra from hot, dense germanium plasma in short pulse laser experiments, High Energy Density Physics, Volume 6, Issue 1, Pages 105-108, ISSN 1574-1818 (2010).
- [6] S. Richardson AWE, Private Communication (2023).
- [7] D.J.R. Swatton AWE, Private Communication (2023).

**UK Ministry of Defence © Crown owned copyright 2023/AWE**

# Measurement of EUV light in laser-produced plasma generated by a 2 $\mu$ m laser on tin droplets

Felix Kohlmeier<sup>1</sup>

<sup>1</sup>*Advanced Research Center for Nanotechnology (ARCNL)*

Extreme ultraviolet (EUV) light is used in the most advanced lithography machines and processes. In these machines, light with a wavelength of 13.5 nm is transported by a series of multi-layer mirrors to resolve ever smaller chip features. To create EUV light in a band of 2 % around the desired wavelength, laser-produced plasma (LPP) on tin droplets is used as a source [1]. Our group at the Advanced Research Center for Nanolithography (ARCNL) is doing research on the related plasma processes.

The LPP plasma is produced in the experimental setup of our research group by a high-intensity laser beam with a wavelength of 1 or 2  $\mu$ m. To study the EUV emission properties, plasma emissions are captured by a variety of sensors [2]. As a main goal of the studies is understanding and optimizing the so-called conversion efficiency into EUV light, a set of EUV photodiodes captures the amount of in-band radiation emitted from the plasma. Additional information on the EUV emission is captured by a transmission grating spectrometer and, in the future, an imaging spectrometer. Using spectroscopy additional information on the emission process can be gained, including, for example, the charge states present in the plasma [3].

A second research topic is the study of debris from the plasma, which can be in the form of charged ions, neutral atoms, or droplet fragments. Debris can impact the mirror collecting the EUV light in lithography machines, reducing the lifetime of the optics. The ionic debris is characterized by a set of retarding field analyzers. With this measurement, the energy spectrum and charge distribution of the ions ejected from the plasma can be reconstructed [4].

The experimental setup is used to improve our understanding of the EUV emission process in LPP of tin droplets. The poster presentation will include our methods and results from recent measurements studying LPPs.

## References

- [1] Oscar O Versolato. *Plasma Sources Science and Technology*, 28(8):083001, 2019. doi:10.1088/1361-6595/ab3302.
- [2] R. Schupp, L. Behnke, J. Sheil, et al. *Physical Review Research*, 3(1):013294, 2021. doi:10.1103/PhysRevResearch.3.013294.
- [3] R. Schupp, F. Torretti, R.A. Meijer, et al. *Physical Review Applied*, 12(1):014010, 2019. doi:10.1103/PhysRevApplied.12.014010.
- [4] L. Poirier, A. Lassise, Y. Mostafa, et al. *Applied Physics B*, 128(7):135, 2022. doi:10.1007/s00340-022-07844-5.

## Edge Toroidal Rotation of Different Ions in ADITYA-U Tokamak

**Ankit Kumar**<sup>1,2</sup>, Aman Gauttam<sup>1</sup>, M.B. Chowdhuri<sup>1</sup>, Dipexa<sup>3</sup>, N.Yadava<sup>4</sup>, N. Ramaiya<sup>1</sup>, K.Shah<sup>5</sup>, Kaushlender Singh<sup>1,2</sup>, K. A. Jadeja<sup>1</sup>, Bharat Hedge<sup>1,2</sup>, Suman Dolui<sup>1,2</sup>, Ashok Kumawat<sup>1,2</sup>, Utsav<sup>1</sup>, S.Patel<sup>3</sup>, Injamul Houqe<sup>1,2</sup>, Soumitra Banerjee<sup>1,2</sup>, Komal<sup>1,2</sup>, G. Shukla<sup>1</sup>, Pramila Gautam<sup>1</sup>, M.Shah<sup>1</sup>, Laxikanta Pradhan<sup>1</sup>, Ankit Patel<sup>1</sup>, K. M. Patel<sup>1</sup>, A. Kanik<sup>3</sup>, Harshita Raj<sup>1</sup>, Suman Aich<sup>1</sup>, Rohit Kumar<sup>1</sup>, Kalpesh Gadoliya<sup>1</sup>, R. Manchanda<sup>1</sup>, R.L. Tanna<sup>1</sup>, Joydeep Ghosh<sup>1,2</sup>

*1Institute for Plasma Research, Bhat, Gandhinagar, Gujarat 382428,*

*2Homi Bhabha National Institute (HBNI), Mumbai 400085,*

*3Pandit Deendayal Petroleum University, Raisan, Gandhinagar 382007, Gujarat,*

*4Oak Ridge Associated Universities, USA*

*5 Princeton Plasma Physics Laboratory, Princeton, USA*

Intrinsic toroidal rotation velocity (self-driven flow) are very crucial in large tokamak like ITER [1,2]. Intrinsic rotation of two different charge states of Carbon ions ( $C^{5+}$  at 529nm,  $C^{2+}$  at 464.74nm) has been studied in the edge region of ADITYA-U tokamak. In several ohmic discharges, these two lines are monitored using 1m high resolution, Czerny-Turner configuration spectrometer. The intrinsic toroidal rotation of these lines are also studied in the presence medium-Z impurity (e.g. Neon, Nitrogen and Argon) seeded discharges. In medium-Z impurity seeded discharges, the toroidal rotation of the seeded impurity ions (e.g. Neon and Argon ions) is compared with the rotation velocity of  $C^{2+}$  and  $C^{5+}$  ions. In all these scenarios, the flow of neutral Hydrogen atoms is also monitored by analysing the shift in  $H_{\alpha}$  line emission (at 656.28nm). All the measurements are done in the flat-top region of discharge. The time resolution as well as the exposure time for the spectroscopic measurement of  $C^{5+}$  ions is 30ms, while for all other spectral lines it is 20ms. It has been observed that the rotation of  $C^{5+}$  ions reverses its direction in the edge region as a result of medium-Z impurity injection (e.g. Neon, Argon).

### References:

- [1] J. E. Rice, Plasma Phys. Controlled Fusion 58, 083001 (2016).
- [2] G. Shukla et al., Nucl. Fusion 59, 106049 (2019).



## A new set of radiative decay rates for forbidden lines in lanthanide ions of interest for kilonova nebular phase studies

**L. Maison**<sup>1</sup>, **P. Palmeri**<sup>1</sup> and **P. Quinet**<sup>1,2</sup>

<sup>1</sup>*Physique Atomique et Astrophysique, Université de Mons – UMONS, B-7000 Mons, Belgium*

<sup>2</sup>*IPNAS, Université de Liège - ULG, B-4000 Liège, Belgium*

On August 17, 2017, the LIGO/Virgo collaboration detected for the first-time a gravitational waves signal (GW170817) associated with a neutron star merger [1]. Following the merger, a large quantity of matter was projected. It was shown that this ejecta was the site of nuclear reactions producing chemical elements heavier than iron such as lanthanides ( $Z = 57-61$ ) [2]. The hot and radioactive material produced a transient electromagnetic phenomenon called kilonova [3]. More recently, in March 2023, astrophysicists detected a gamma ray burst associated with what could be a merger of compact objects followed by a transient afterglow. After analysing the spectra, they found some similarity with the AT2017gfo kilonova spectra suggesting the presence of such phenomena. The particularity with this kilonova event is that the spectrum has been recorded, by the Near Infrared Spectrograph (NIRSpec) onboard the James Webb Telescope (JWST), at late time after the merger [4]. At these times, the kilonova is said to be in his nebular phase. Conditions are such that the temperature is really low and the ionization stage does not exceed the doubly charged species. Only low-lying levels, such as metastable levels, are populated giving rise to so-called emission forbidden lines, such as the magnetic dipole (M1) and electric quadrupole (E2) transitions. So, for example, the analysis of the late time spectrum showed some spectral features coming from forbidden transitions of heavy elements like Te III [5]. Element identification in nebular phase spectra is quite challenging since atomic data and especially forbidden line lists for heavy elements are scarce in the literature.

In order to extend the study of kilonovae in their nebular phase, we carried out new calculations of transition probabilities for M1 and E2 lines between low-lying levels in singly and doubly ionized lanthanide atoms. Given the lack of data in the literature, two theoretical methods were used in this work to model the atomic structure of these ions and to compute the radiative parameters. The first one is the fully-relativistic Multi-Configurational-Dirac-Hartree-Fock (MCDHF) method [6] with the GRASP2018 code [7]. The computed values were then compared to the results deduced from pseudo-relativistic Hartree-Fock (HFR) calculations [8] in order to check their reliability. This allowed us to obtain a new consistent set of atomic data allowing astrophysicists to study the infrared spectrum of kilonovae in their nebular phase.

[1] B. P. Abbott, *et al.*, Phys. Rev. Lett. **119**, 161101 (2017).

[2] E. Pian, *et al.*, Nature **551**, 67-70 (2017).

[3] B. D. Metzger, Living Rev. Relativ. **20**, 3 (2017).

[4] J. H. Gillanders, *et al.*, arXiv e-print: arXiv:2308.00633 (2023).

[5] A. Levan, *et al.*, arXiv e-print: arXiv:2307.02098v1 (2023).

[6] I. P. Grant, “*Relativistic quantum theory of atoms and molecules: theory and computation*”, New-York: Springer (2007).

[7] C. Froese Fischer, *et al.*, Comput. Phys. Commun. **237**, 184 (2019).

[8] R. D. Cowan, “*The theory of atomic structure and spectra*”, Berkley: University of California Press (1981).

## Numerical investigation of ionization dynamics in intense laser-heated argon plasma using the NLTE model

M. S. Cho<sup>1</sup>, A. L. Milder<sup>2</sup>, W. Rozmus<sup>3</sup>, H. P. Le<sup>1</sup>, and M. E. Foord<sup>1</sup>

<sup>1</sup>*Lawrence Livermore National Laboratory, Livermore CA, USA*

<sup>2</sup>*Laboratory for Laser Energetics, Rochester NY, USA*

<sup>3</sup>*University of Alberta, Edmonton AB, Canada*

The ionization dynamics of laser-generated plasmas play a crucial role in our understanding of larger macroscopic systems. The non-local thermodynamic equilibrium (NLTE) model stands out as a primary method for evaluation of ionization for given plasma conditions. This model identifies various ionization processes and allows calculation of the distribution of ionization states. Here, the ionization dynamics of underdense argon gas are presented. Time dependent calculations of argon gas ionized by an intense laser ( $I=10^{15}$  W/cm<sup>2</sup>) to a temperature of 700eV and density of  $2.5\times 10^{19}$  cm<sup>-3</sup> show an average ionization state lower than that predicted by steady state calculations. Modelling in this regime also shows ionization is dominated by two-stage processes where electrons are excited to high n-number primarily through collisional excitation and dielectric recombination and then ionized through photoionization.

## Soft x-ray emitting laser-produced plasmas: Advances in imaging, spectroscopy and simulation techniques

K. Mongey, R. Brady, B. Delaney, E. Sokell, F. O' Reilly

*School of Physics, University College Dublin, Belfield, Dublin 4, Ireland*

kevin.mongey@ucdconnect.ie

The development and deployment of laboratory-based soft x-ray light sources is a growing research activity - for some applications such as soft x-ray tomography[1], they offer an affordable and compact alternative to the current gold standard of soft x-ray production via synchrotron and Free Electron Laser facilities[2]. A common alternative method x-ray generation via creation of a laser-produced plasma (LPP)[3]. The subsequent x-ray emission generated can be tuned by appropriate choice of laser wavelength, energy, pulse duration and target material.

Presented here are recent developments in experimental characterisation and modelling of micrometer scale soft x-ray emitting LPPs, generated via the irradiation of select metallic targets using a tightly focused Nd:YAG 1064 nm 5 nanosecond laser. The motivation is to reveal the spatial and spectral behaviours of these tiny plasmas with the ultimate goal of increasing radiance for source optimisation. We present unique deconvolution techniques applied to pinhole images of generated soft x-ray emitting plasmas, from which the true size of the plasma can be inferred, which cannot be inferred directly from pinhole imaging due to diffractive blurring. We show the design and use of a compact and cost-effective soft x-ray spectrometer. We show that similar spectral information can be extracted from the spatial imaging of these plasmas. Finally, we present developments in the simulation of these small-scale, x-ray plasmas via the single-temperature, single-fluid hydrodynamics code with radiation transport, RALEF-2D[4], which shows promising results in the ability of predictive modelling techniques.

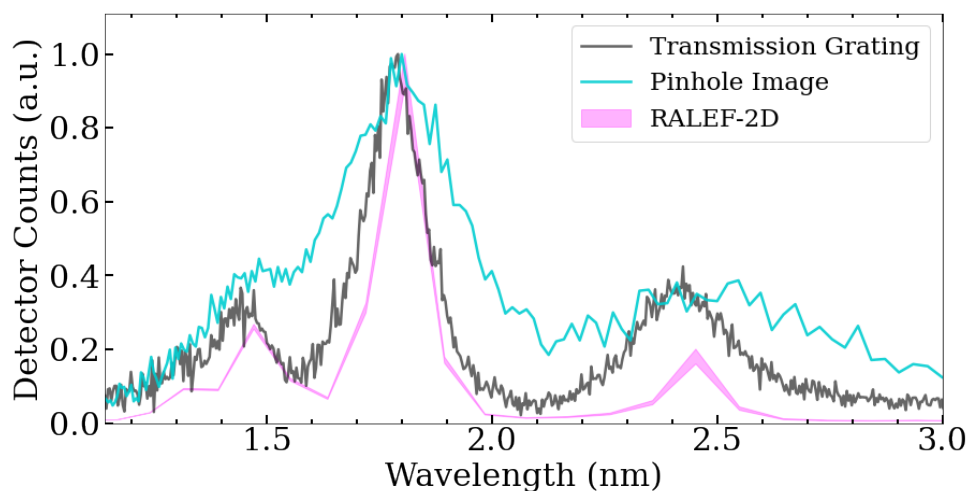


Figure 1: Soft x-ray spectrum of tin shown from the transmission grating spectrometer in black, pinhole image in blue and RALEF-2D in magenta.

This work is supported by Science Foundation Ireland (SFI), via the *Frontiers for the Future Programme* Award under grant 19/FFP/6795.

- [1] K. Fahy, et al., *Journal of Physics: Photonics*, **3**, 031002 (2021).
- [2] D. Bleiner, *Spectrochimica Acta Part B: Atomic Spectroscopy*, **181**, 105978 (2021).
- [3] G. O'Sullivan, et al., *Journal of Physics B* **48**, 144025 (2015).
- [4] M. M. Basko, J. Maruhn, and A. Tauschwitz, *GSI Rep.* **1**, 410 (2010).

## Poster on inferring the role of plasma-neutral interactions in tokamak divertors using hydrogen emission spectroscopy

**Kieran A. Murray**<sup>1</sup>

<sup>1</sup>(*PHD student UKAEA*)

Power exhaust in the divertor region is a critical challenge in magnetic confinement fusion devices. Plasma-neutral interactions, including atomic & molecular interactions that result in plasma chemistry, can have a major impact on the hydrogenic radiation as well as the physics in the divertor region.

Atomic hydrogen emission in the divertor occurs from three different processes occur: electron-impact excitation of hydrogen atoms, electron-ion recombination of hydrogen ions, and plasma-molecular chemistry resulting ultimately in excited hydrogen atoms. This plasma-chemistry arises from interactions between the plasma and vibrationally excited molecules, resulting in the formation of molecular ions that interact with the divertor plasma.

In my poster, I will show a Bayesian Markov-Chain Monte Carlo (MCMC) approach to infer quantitative information on these processes using measurements of the hydrogen Balmer lines ( $n=3,4,5$ ), including ion sources & sinks as well as hydrogenic radiation inferences in the form of Probability Density Functions. This approach works by separating the ratios of these three processes, which then enables us to calculate the divertor chemistry. To do this, we use data from the ADAS collisional-radiative model for atomic processes and from the Yacora On The Web collisional-radiative model for molecular interactions. Additionally, my poster will explore how such interactions impact the divertor plasma, showing experimental data from the MAST-U Super-X divertor where plasma chemistry has a profound impact on the divertor behaviour.

Abstract for Joint ICTP-IAEA School on Data for Modelling Atomic and  
Molecular Processes in Plasmas | (smr 3924)

## **ELECTRON INTERACTIONS WITH FLUOROMETHANES**

**Smruti Parikh<sup>1\*</sup>, Minaxi Vinodkumar<sup>2</sup> and Chetan Limbachiya<sup>1</sup>**

<sup>1</sup>*The Maharaja Sayajirao University of Baroda, Vadodara-390 001, India*

<sup>2</sup>*V.P. and R.P.T.P. Science college, Vallabh Vidyanagar-388120, India*

It is fascinating to see the growing interest in the study of electron scattering by fluoromethanes and its diverse applications in various fields. The importance of electron scattering studies extends to various scientific and industrial domains. In particular, the urgent need for cross-section data for electron scattering from partially fluorinated methanes ( $\text{CH}_2\text{F}_2$ ,  $\text{CH}_3\text{F}$ ,  $\text{CHF}_3$ ) is required, especially in plasma processing, material sciences, and earth sciences [1]. These partially fluorinated methane gases, being considered "environmentally acceptable, next-generation plasma-processing gases," are of interest due to their potentially shorter atmospheric lifetimes compared to  $\text{CF}_4$  [2]. Hence, in the present work we studied the electron interactions with fluoromethanes, viz.,  $\text{CH}_3\text{F}$ ,  $\text{CH}_2\text{F}_2$  and  $\text{CHF}_3$  for an extensive impact energy range 0.1 eV to 5000 eV. For the low energy calculations, we employed the R-matrix formalism [3] and for intermediate to high energy calculations, Spherical Complex Optical Potential approach [4] in conjunction with Complex Scattering Potential-ionization contribution method has been utilized [5]. Various cross-sections (momentum transfer, differential, ionization, excitation, total inelastic, elastic etc.) for various elastic and inelastic molecular processes have been quantified.

[1] L. G. Christophorou, J. K. Olthoff, and M. V. V. S. Rao, J. Phys. Chem. Ref. Data **26**, 1 (1997).

[2] L. G. Christophorou, J. K. Olthoff, and M. V. V. S. Rao, J. Phys. Chem. Ref. Data **25**, 1341 (1996).

[3] M. Vinodkumar, C. Limbachiya, A. Barot, and N. Mason, Phys. Rev. A **86**, 012706 (2016).

[4] S. Parikh, M. Vinodkumar, and C. Limbachiya, Chem. Phys. **565**, 111766 (2023).

[5] S. Parikh, and C. Limbachiya, Radiat. Phys. Chem. **208**, 110940 (2023).

# Enhancing Quantitative Analysis efficiency with Deep Learning Neural Network Coupled Laser-Induced Breakdown Spectroscopy

Leya Pauly<sup>1</sup>, and K. K. Anoop<sup>1\*</sup>

<sup>1</sup>*Department of Physics, Cochin University of Science and Technology, Kochi-682022, India.*

*\*Email: anoopkk@cusat.ac.in*

Laser-Induced Breakdown Spectroscopy (LIBS) is an analytical method rooted in Atomic Emission Spectroscopy (AES). The traditional approach to quantitative analysis in LIBS, involving calibration curves, can be quite cumbersome [1]. However, in recent years, there has been significant growth in the integration of machine learning algorithms with LIBS for quantitative analysis [2]. Spectral quantitative analysis in conjunction with conventional supervised machine learning techniques such as linear regression, support vector regression (SVR) and so on, has showcased impressive capabilities in efficiently identifying the composition of elements present in samples [3]. Among the conventional machine learning algorithms, Deep Learning Neural Network (DNN) coupled LIBS is a promising analytical tool developed for the efficient compositional analysis [4]. In this work, we have proposed a deep learning neural network (DNN) model for the efficient quantitative analysis of Bronze (Cu-Sn) and Brass (Cu-Zn) alloys and has worked on improving the quantitative results by increasing the number of simulated spectra used for training. The simulation method allows obtaining synthetic spectra for training the model for different concentration of elements for a range of electron temperature and density [5]. This study suggests that employing DNN-supported LIBS is a promising analytical tool for multi-elemental compositional analysis.

## References

- [1] Ciucci, A., Corsi, M., Palleschi, V., Rastelli, S., Salvetti, A., Tognoni, E., *Appl Spectrosc.* **53**, 960–964 (1999).
- [2] Ruan, F., Qi, J., Yan, C., Tang, H., Zhang, T., Li, H., *J. Anal. At. Spectrom.* **32**, 2194–2199 (2017).
- [3] Sun, C., Tian, Y., Gao, L., Niu, Y., Zhang, T., Li, H., Zhang, Y., Yue, Z., *Sci Rep.* **9**, 1–18 (2019).
- [4] Van Den Eynde, S., Diaz-Romero, D.J., Zaplana, I., Peeters, J., *SSRN Journal.* (2022).
- [5] Sivadas, M.S.S., John, L.M., Anoop, K.K., *IOP Conf. Ser.: Mater. Sci. Eng.* **1221**, 012027 (2022).

## Unveiling the non-linear Zeeman effect in isotopes of krypton and xenon at the linear plasma device PSI-2

**M. Sackers<sup>1</sup>, O. Marchuk<sup>1</sup>, Dipti<sup>2</sup>, S. Ertmer<sup>1</sup>, Yu. Ralchenko<sup>3</sup>, and A. Kreter<sup>1</sup>**

<sup>1</sup>*Forschungszentrum Jülich GmbH - Institut für Energie- und Klimaforschung - Plasmaphysik, Partner of the Trilateral Euregio Cluster (TEC), 52425 Jülich, Germany*

<sup>2</sup>*International Atomic Energy Agency, Vienna, Austria*

<sup>3</sup>*National Institute of Standards and Technology - Atomic Spectroscopy Group, 20899 Gaithersburg, USA*

Isotopic broadening alters the line shape of atomic transitions and contributes noticeably to the laser absorption spectra of neutral Kr and Xe investigated at the linear plasma device PSI-2. Of high interest are the odd-numbered isotopes having a nonzero nuclear spin resulting in the hyperfine interaction. The main challenge in analyzing such isotopes is that the hyperfine and Zeeman terms can be of the same order of magnitudes, rendering conventional weak field and strong approximation formulas inadequate for analysis.

The magnetic field at PSI-2 of  $< 90$  mT creates such conditions for the Kr I 760.4 nm, Kr I 785.7 nm, and Xe I 764.4 nm lines. This contribution shows how to correctly account for the Zeeman effect by using a Hamiltonian containing both hyperfine and Zeeman interaction terms as the perturber. Standard atomic physics procedures allow us to derive the energy eigenvalues and relative intensities. Crucially, the theoretical analysis is backed by experimental data, confirming the validity of the methodology in modeling observed spectral features.

## Design of TALIF and CARS Diagnostics for Measuring Atomic and Molecular Hydrogen Densities in Divertor-relevant Plasmas

K. Schutjes<sup>1\*</sup>, K.J. Loring<sup>1,2</sup>, I.G.J. Classen<sup>1</sup>, J. Vernimmen<sup>1</sup>, H.J. van der Meiden<sup>1</sup>,  
and the Magnum-PSI team<sup>1</sup>

<sup>1</sup>*Dutch Institute For Fundamental Energy Sources (DIFFER), Eindhoven, The Netherlands*

<sup>2</sup>*Stanford University, Palo Alto, California, United States of America*

One of the biggest challenges of a reliable fusion reactor is the handling of large heat and particle loads on the divertor wall. Key to reducing these loads is by plasma detachment, in which a large range of processes occur between the plasma and the neutral background [1,2]. Atomic and molecular processes largely determine the plasma dynamics, which is why these particles are often studied in divertor research [1,2]. However, measurements on electronic ground state densities for atoms and molecules are lacking for divertor-relevant plasmas. We will use active laser spectroscopy, using TALIF and CARS, to measure these densities.

To measure the atomic hydrogen ground state density, a TALIF setup has been developed to allow measurements in the linear plasma device UPP. UPP is able to create divertor-relevant plasma conditions ( $n_e \approx 10^{20} \text{ m}^{-3}$ ,  $T_e < 5 \text{ eV}$ ). Nanosecond laser pulses in the 204-206 nm range are used to excite hydrogen from the ground state, and fluorescence was monitored with a gated ICCD camera. The first spatially-resolved measurements in UPP were performed and will be presented.

A CARS setup has been designed and is tested on a gas cell filled with H<sub>2</sub> gas. Work is currently underway to apply this setup in the linear plasma device UPP. Signal is generated using focused nanosecond laser pulses, and is detected with a gated ICCD camera. Two lasers are used: a seeded Nd:YAG (532 nm, 6 ns pulse, 0.005 cm<sup>-1</sup> linewidth) and a dye laser (660-685 nm, 6 ns pulse, ~0.1 cm<sup>-1</sup> linewidth). Spatially-resolved measurements of the lower rovibrational population have been performed and the first preliminary results will be presented.

[1] A. Loarte, *et al.*, Nucl. Fusion 47 S203 (2007). DOI: 10.1088/0029-5515/47/6/S0

[2] S.I. Krasheninnikov and A.S. Kukushkin, J. Plasma Phys. 83 (2017). DOI:10.6100/IR58304

\*Presenting author: k.schutjes@diffier.nl



## Multipole rate coefficients for excitation of Fe XIII by isotropic Maxwellian electrons

A. F. Sekkal-Haddouche, M. K. Inal, and M. Benmouna

Department of Physics, Faculty of Sciences, University of Tlemcen, 13000 Tlemcen, Algeria

Knowledge of the usual rate coefficients for electron-impact excitation of ions between fine-structure levels may not be sufficient to interpret line emission from plasmas even with an isotropic Maxwellian electron distribution. This is particularly true when the line emission is due both to collisions with isotropic electrons and photoexcitation by anisotropic radiation coming from an external source [1], as it occurs, for example, in the solar corona under irradiation by the photosphere. For the analysis of line emission from plasmas under those conditions, the multipole rate coefficients  $C^K$  for excitation by isotropic electrons are needed. The possible values of the quantum number  $K$  are  $0, \dots, 2 \min(J_i, J_f)$ ,  $J_i$  and  $J_f$  being the total angular momenta of initial and final levels involved in the excitation. The calculation of  $C^K$  requires integration over an energy electron distribution of the multipole collision strength  $\Omega^K$  given by [2]

$$\Omega^K = \sum_{\lambda} (-1)^{J_i+J_f+K+\lambda} \left\{ \begin{array}{ccc} J_i & J_i & K \\ J_f & J_f & \lambda \end{array} \right\} \Omega_{\lambda}, \quad (1)$$

where  $\{ \}$  denotes a  $6j$  symbol and  $\Omega_{\lambda}$  is the  $\lambda$  component of the usual collision strength  $\Omega$ , i.e.,  $\Omega = \sum_{\lambda} \Omega_{\lambda}$ ,  $\lambda$  being the multipole order of the Coulomb interaction between electrons.

Assuming a Maxwellian distribution for the electrons, we have calculated the  $C^K$  for transitions in the Si-like Fe XIII ion between levels of the  $3s^23p^2$  ground configuration and from  $3s^23p^2$  to  $3s^23p3d$  levels for temperatures  $T_e$  in the range  $(0.7-5) \times 10^6$  K. These transitions are of interest in solar corona diagnostics based on the infrared magnetic-dipole lines  $3p^2^3P_1 \rightarrow 3p^2^3P_0$  and  $3p^2^3P_2 \rightarrow 3p^2^3P_1$  and extreme ultraviolet optically-allowed lines  $3p3d^3P_1 \rightarrow$

$3p^2^3P_0$  and  $3p3d^3D_{2,3} \rightarrow 3p^2^3P_2$ . Computations of  $\Omega^K$  have been carried out at several scattered-electron energies from 0.01 eV up to 2 keV, using a modified version [2, 3] of the relativistic distorted-wave program of the Flexible Atomic Code [4]. Configuration interactions among  $3s^23p^2$ ,  $3s3p^3$ ,  $3s^23p3d$ ,  $3p^4$ ,  $3s3p^23d$  and  $3s^23d^2$  configurations were included in the computations.

As an example, we give in figure 1 the results for the transitions  $3p^2^3P_2 \rightarrow 3p3d^3P_1$ ,  $3p^2^3P_1 \rightarrow 3p3d^3D_2$ , and  $3p^2^3P_2 \rightarrow 3p3d^3D_3$  including all the contributing  $\lambda$ -terms in the summation of equation (1). It is seen that the curves  $C^K$  versus  $T_e$  are nearly parallel exhibiting a broad peak at practically the same temperature about  $2 \times 10^6$  K. If one takes into account only the dominant  $\lambda = 1$  term, one finds that  $C^{K \neq 0}$  increases very slightly, by less than 3% for the three transitions. This is consistent with the quasi-parallel trends of the  $C^K$  curves observed in figure 1 for each transition, considering the fact that  $C^{K \neq 0}$  is proportional to  $C^0$ .

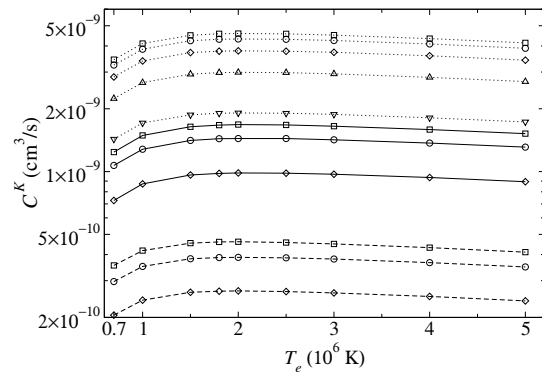


Figure 1:  $C^K$  ( $K=0-2$ ) for  $3p^2^3P_2 \rightarrow 3p3d^3P_1$  (solid curves) and  $3p^2^3P_1 \rightarrow 3p3d^3D_2$  (dashed curves), and  $C^K$  ( $K=0-4$ ) for  $3p^2^3P_2 \rightarrow 3p3d^3D_3$  (dotted curves).  $\square$ :  $C^0$ ,  $\circ$ :  $C^1$ ,  $\diamond$ :  $C^2$ ,  $\triangle$ :  $C^3$ ,  $\nabla$ :  $C^4$ .

- [1] L. Belluzi, E. Landi Degl'Innocenti, J. Trujillo Bueno, *Astron. Astrophys.* **551**, 84 (2013).
- [2] A. F. Sekkal-Haddouche, M. K. Inal, M. Benmouna, *Eur. Phys. J. D* **77**, 148 (2023).
- [3] M. Belabbas, M. K. Inal, M. Benmouna, *Phys. Rev. A* **104**, 042818 (2021).
- [4] M. F. Gu, *Can. J. Phys.* **86**, 675 (2008).

# Electron and Positron impact partial ionization cross sections of diatomic molecules present in the interstellar medium

Suriyaprasanth S<sup>1</sup>, Geetha D, Snigdha Sharma, and Dhanoj Gupta<sup>2</sup>

*Department of Physics, School of Advanced Sciences, Vellore Institute of Technology, Vellore, TN - 632014, India.*

Looking at the starry night and wondering “Where and How did everything begin?” is always fun and intriguing for us. Although the question might look simple and clumsy, the answer looks far more complex and yet unknown. Mysteries of the origins of life from space are due to chemical processes that happen in the interstellar molecular clouds present in the interstellar medium (ISM) and the protoplanetary disks. The reason is, that these prime locations are rich in materials or compounds, and interstellar travelers like comets, clouds of dust, and meteors act as a vector in delivering such compounds to new environments such as the planetary atmosphere and then to the surface of planets itself, directly contributing to the development of life crucially [1]. Recently, Sanchez *et al.* [2] discussed the importance of LiX (X = H, He) and HeH in the ISM. The 2021 census of Brett A. McGuire [3] also features an extensive variety of molecules including diatomic species which were detected with radio astronomy in the ISM clouds, these cold clouds house several molecules in the gas phase, and ionization is one of the important processes due to the scattering of electrons, positrons, and photons in such an atmosphere. Albeit in literature, there exist numerous studies on elastic and inelastic scattering processes for known targets such as O<sub>2</sub>, H<sub>2</sub>, N<sub>2</sub>, C<sub>2</sub>, CH, CO, NH, and CN which were also detected at the ISM. However, for the other diatomic targets that were present in the 2021 census, we could not find any study on the PICS for these molecules which could give us a better insight into the chemistry of extreme environments. In this work, we study the total ionization cross sections (TICS) and partial ionization cross sections (PICS) [4, 5] for electron and positron impact on several diatomic molecules detected in the ISM employing the Binary Encounter Bethe (BEB) model [6] and references therein. In Figure. 1, We have shown the electron and positron TICS of the LiX group. So, we plan to present the electron/positron TICS and PICS to all the molecules from the aforementioned works of Brett A. McGuire and Sanchez.

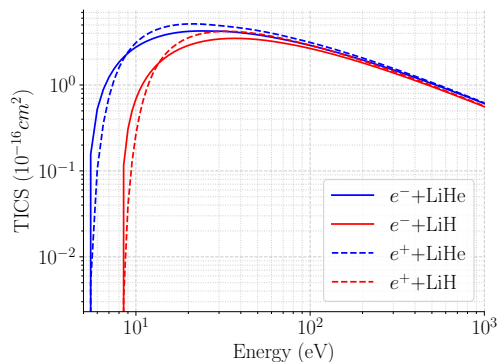


Figure 1: Electron and Positron impact TICS of LiHe (blue color) and LiH (red color)

- [1] Sandford, S. A., *et al. Chem. Rev.* **120**, 11, 4616. (2020).
- [2] González-Sánchez, L., *et al. Phys. Chem. Chem. Phys.* **25**, 23370. (2023).
- [3] Brett A. McGuire *ApJS.* **259**, 30. (2022).
- [4] Huber, S. E., *et al. J. Chem. Phys.* **150**, 024306. (2019).
- [5] Graves, Vincent., *et al. J. Phys. B: At. Mol. Opt. Phys.* **54**, 235203. (2021).
- [6] Suriyaprasanth, S., *et al. Atoms.* **11**, 137. (2023).

<sup>1</sup>Presenting author: suriyaprasanth.s@vit.ac.in

<sup>2</sup>Corresponding author: dhanoj.gupta@vit.ac.in

## Spectral properties of plasma embedded He-like Ar XVII under the influence of external magnetic field

**Shivankar<sup>1</sup>, Narendra Kumar<sup>1</sup>, Alok Kumar Singh Jha<sup>1</sup>, Man Mohan<sup>2</sup>**

<sup>1</sup>*School of Physical Sciences, Jawaharlal Nehru University, New Delhi, India*

<sup>2</sup>*Department of Physics and Astrophysics, University of Delhi, Delhi, India*

The atomic structure calculations and radiative properties of He like Ar XVII in the presence of dense plasma environment and external magnetic field have been presented. For this purpose, the relativistic configuration interaction method (RCI) by incorporating the generalized b-potential and external magnetic field has been implemented. In the case of free atoms or ions, our calculated results are in good agreement with NIST and other available data. Plasma screening effect on  $1s^2\ ^1S_0 \rightarrow 1s2p\ ^3P_1$  and  $1s2p\ ^1S_0 \rightarrow 1s2p\ ^1P_1$  transitions of Ar XVII ion in the presence of an external magnetic field has been investigated. The Zeeman splitted energies and the excitation energies of Ar XVII ion for the magnetic sublevels  $1s2p\ ^3P_0$  ( $M_j = 0$ ),  $^3P_1$  ( $M_j = 0, \pm 1$ ),  $^3P_2$  ( $M_j = 0, \pm 1, \pm 2$ ),  $^1P_1$  ( $M_j = 0, \pm 1$ ) has been calculated and the variation in the binding energy of Ar XVII in plasma environment and magnetic field has been observed. Our results will be useful in the modeling and diagnostics of laboratory and astrophysical plasmas.

### References

- [1]. M. F. Gu, Can. J. Phys. 86, 675-689 (2008).
- [2]. X. Li, F. B. Rosmej, V. S. Lisitsa, V.A. Astapenko, Phys. Plasmas 26, 033301 (2019).
- [3]. A. K. Singh, D. Dawra, M. Dimri, A. K. S. Jha, R. K. Pandey, M. Mohan, Phys. Lett. A 384, 126369 (2020).
- [4]. Z. B. Chen, Y. Y. Qi, H. Y. Sun, P. F. Liu, K. Wang, Jour. Quan. Spect. & Rad. Transfer 277, 107999 (2022).

## He / Ne Beam Line Ratio Spectroscopy to Investigate Plasma Boundary of Wendelstein 7-X Stellarator Fusion Experiment

Foissal B. T. Siddiki<sup>1</sup>, T. Barbui<sup>2</sup>, E. Flom<sup>1,3</sup>, O. Schmitz<sup>1</sup>, M. Krychowiak<sup>3</sup>, and W7-X Team

<sup>1</sup> *University of Wisconsin-Madison, USA*

<sup>2</sup> *Princeton Plasma Physics Laboratory, USA*

<sup>3</sup> *Max Planck Institute for Plasma Physics, Germany*

Heat and particle transport in the plasma boundary region, also known as the scrape-off layer (SOL) situated beyond the last closed flux surface in a fusion device, significantly influences the performance of the divertor, which serves as the heat and particle exhaust system. In order to optimize the divertor concept, it is crucial to gain insights into the transport phenomena within the SOL, achieved through studying plasma parameters such as electron temperature ( $T_e$ ) and density ( $n_e$ ). The Wendelstein 7-X (W7-X) stellarator has ten novel island divertor units intersecting the plasma edge [1]. As a way of measuring the basic plasma parameters in the SOL, diagnostic systems used consist of a gas injection system and multiple high resolution spectrometers installed in the mid-plane and in front of the W7-X divertor. The gas injection system injects helium (He), neon (Ne) or a mixture of both, and the array of spectrometers can measure their respective spectral lines [2]. Line ratio spectroscopy based on a collisional radiative model is used to infer the  $n_e$  and  $T_e$ . The He beam diagnostic at W7-X has been well validated and extensively used to map the plasma parameters in the island divertor, and the addition of Ne will allow for more accurate mapping of the low temperature regime of the edge ( $T_e < 5$  eV) [3] [4]. The temperature and density profile presented here is measured above the horizontal divertor target in various conditions including detached and impurity-seeded plasmas.

[1] Renner, H., et al. No. IAEA-CSP-19/CD. 2003.

[2] Barbui, Tullio, et al. J. of Ins. 14.07 (2019): C07014.

[3] Barbui, Tullio, et al. Nuclear Fusion 60.10 (2020): 106014.

[4] Krychowiak, Maciej, et al. Plasma Physics and Controlled Fusion 53.3 (2011): 035019.

## Theoretical Investigation of anomalous Intensity Ratio of Spectral Lines of at 18.03 and 18.79 nm of Ar<sup>13+</sup> ion in ADITYA-U tokamak.

**Gajendra Singh<sup>1</sup>, M. B. Chowdhuri<sup>1</sup>, J. Ghosh<sup>1,2</sup>, Aman Gauttam<sup>1</sup>, Dipexa Modi<sup>3</sup>, S. Patel<sup>3</sup>, Nandini Yadava<sup>4</sup>, N. Ramaiya<sup>1</sup> and S. K. Pathak<sup>1,2</sup>**

<sup>1</sup>*Institute for Plasma Research, Bhat, Gandhinagar 382 428, India*

<sup>2</sup>*Homi Bhabha National Institute, Anushaktinagar, Mumbai 400 094, India*

<sup>3</sup>*Pandit Deendayal Energy University, Raision, Gandhinagar 382 007, India*

<sup>4</sup>*Oak Ridge Associated Universities, Oak Ridge, Tennessee 37831, USA*

Vacuum ultraviolet (VUV) spectroscopy on ADITYA-U tokamak is carried out to understand the impurity behaviour in the plasma. Argon impurity transport study in ADITYA-U tokamak has revealed the role of inward pinch in the core argon transport [1]. To carry out such study, the observed VUV lines from Ar<sup>13+</sup> ions at 18.79 nm ( $2s^2 2p^2 P_{3/2} - 2s 2p^2 P_{3/2}$ ) and Ar<sup>14+</sup> ions at 22.11 nm ( $2s^2 1S_0 - 2s 2p^1 P_1$ ) are utilized. However, it has been observed that the intensity of 18.79 nm line of Ar<sup>13+</sup> ions is orders of magnitude greater than the resonance lines at 18.03 nm ( $2s 2p^2 P_{3/2} - 2s^2 2p^2 P_{1/2}$ ) and 18.34 nm ( $2s 2p^2 P_{1/2} - 2s^2 2p^2 P_{1/2}$ ). The similar feature has also been observed in few other tokamaks in the past [2-3]. However, no attempts have been made in the past to explain this anomaly. Present theoretical study aims to explain the anomaly associated with this feature as it is normally believed that the resonance lines having transition to ground state level  $2s^2 2p^2 P_{1/2}$  are more stronger than the lines having transition to the lower level at excited state.

In this present work, the theoretical line intensity calculations of all the above three lines of Ar<sup>13+</sup> ion have been carried out. Here, first the photon emission coefficients (PEC) are evaluated for all three lines using the collisional radiative model (CRM) of Atomic Data and Analysis Structure (ADAS) database. The experimental intensities of all three lines are matched with theoretical calculations to find out the processes responsible for higher intensity of 18.79 line as compared to 18.03 line. It has been found through the theoretical estimation that higher absorption oscillation strength of ( $2s^2 2p^2 P_{3/2} - 2s 2p^2 P_{3/2}$ ) transition is the reason behind the observation of anomalous intensity ratio between 18.79 and 18.03 nm line.

[1] K Saha, J Ghosh et al. Scientific Reports **13**, 16087 (2023).

[2] Träbert, Elmar, et al. The Astrophysical Journal **148**, 865.2 (2018).

[3] Katai, R., S. Morita, and M. Goto. Journal of Quantitative Spectroscopy and Radiative Transfer **107**, 120-140 (2007).

## Opacity calculations of various elements at a variety of plasma conditions using the improved FLYCHK code

**Jang Hyeob Sohn<sup>1</sup>, Hyun-Kyung Chung<sup>2</sup>, Byoung-Ick Cho<sup>1,3</sup>, and Sang June Hahn<sup>4</sup>**

<sup>1</sup>*Department of Physics and Photon Science, Gwangju Institute of Science and Technology (GIST), Gwangju 61005, South Korea*

<sup>2</sup>*National Fusion Research Institute, Daejeon 34133, South Korea*

<sup>3</sup>*Center for Relativistic Laser Science, Institute for Basic Science (IBS), Gwangju 61005, South Korea*

<sup>4</sup>*Department of Physics, Chung-Ang University, Seoul 06974, South Korea*

Opacity, which describes the extent to which the radiation is absorbed and scattered in the material, is essential in understanding the fundamental physical properties of high-energy-density(HED) and astrophysical plasmas. FLYCHK, a collisional-radiative code, has been used to calculate the opacities of HED plasmas under a wide range of conditions due to the simplicity and availability of the code[1,2]. However, it has been confirmed that the FLYCHK opacity has limitations in strongly coupled plasmas due to the problem of free-free opacity formalism[3,4]. In this research, we improve the free-free opacity calculation model of FLYCHK and generate opacities of various elements at a variety of plasma conditions. The FLYCHK opacities agree well with those obtained by the Los Alamos opacity code ATOMIC[5].

[1] H-K. Chung, et al., High Energy Density Phys. **1**, 3-12 (2005).

[2] H-K. Chung, M. H. Chen, and R. W. Lee., High Energy Density Phys. **3**, 57-64 (2007).

[3] M. S. Cho, et al., J. Quant. Spectrosc. Radiat. Transf. **257**, 107369 (2020).

[4] M. S. Cho, et al., J. Korean Phys. Soc. **78**, 1072-1083 (2021)

[5] J. Colgan, et al., Astrophysical J. **817**, 116 (2016): 116.

## Diffraction Order Penalization to Improve Spectrometer Calibrations

**Hunter Staiger<sup>1,2</sup>, Endre Takacs<sup>1,2</sup>, and Yuri Ralchenko<sup>2</sup>**

<sup>1</sup>*Department of Physics and Astronomy, Clemson University, Clemson, 29631, SC, USA*

<sup>2</sup>*National Institute of Standards and Technology, Gaithersburg, 20899, MD, USA*

Calibration in diffracted spectroscopy typically depends on identifying strong, well-known lines in the recorded spectra and fitting a calibration function to them. We outline a novel method (order penalization) for improving spectroscopic calibrations by extending non-linear least squares fitting of the calibration curve. The method introduces an extra term into the minimized quantity that penalizes disagreement in the positions of spectral lines observed in multiple diffraction orders. The primary advantage of this method is that the lines used do not have to be identified, except for establishing the fact that they are different orders of the same line. This increases the number of constraints on the calibration curve, potentially in spectral regions where no regular calibration lines are available. The mathematical basis of this method is described, and the performance of this method is evaluated on simulated data and experimental data from the National Institute of Standards and Technology (NIST) Electron Beam Ion Trap. We demonstrate the effectiveness of the method on the spectra of highly charged Ag-like Re28+ and nearby charge state ions.

## Development of Capacitively Coupled Radio Frequency Discharge Plasma Device for the Validation of Supersonic Molecular Beam Diagnostics using Collisional-Radiative Model.

Varsha S<sup>1,2</sup>, Prabhakar Srivastav<sup>1</sup>, Milaan Patel<sup>2</sup>, Vishnu Chaudhari<sup>1</sup>, Amit Kumar<sup>1</sup>  
and Jinto Thomas<sup>1,2</sup>

<sup>1</sup> *Institute for Plasma Research (IPR), Bhat P.O. Gandhinagar, Gujarat, 382428*

<sup>2</sup> *Homi Bhabha National Institute, Training School Complex, Anushaktinagar, Mumbai, 400094, India.*

Molecular beam diagnostics, such as helium beams, can be used to profile plasma density and temperature at the edge of the tokamak plasma [3]. A Supersonic Molecular Beam Injection (SMBI) system has been designed and validated for this purpose [1]. The interaction of the beam with the plasma can be studied using a dedicated high frequency capacitive discharge (CCRF) plasma system, in which other diagnostics such as Langmuir probe etc. can be used to validate the measured parameters. Estimation of plasma parameters using helium beam diagnostics is based on collisional radiative (CR) modelling of the spectroscopic emission resulting from the interaction of the SMB with the plasma [4]. A CCRF plasma is generated in a controlled environment using a 13.56 MHz RF source in a glass chamber and characterised using probes [2]. In this poster, an overview of the CCRF plasma system and the plans to integrate the SMBI into it are discussed.

- [1] M. Patel, J. Thomas, and H. C. Joshi, Flow Characterization of Supersonic Gas Jets: Experiments and Simulations, *Vacuum* **192**, 110440 (2021).
- [2] I. D. Sudit and F. F. Chen, Rf Compensated Probes for High-Density Discharges, *Plasma Sources Sci. Technol.* **3**, 162 (1994).
- [3] E. Wolfrum, M. Griener, M. Cavedon, J. M. Muñoz Burgos, O. Schmitz, U. Stroth, and the ASDEX Upgrade Team, "First results from the thermal helium beam diagnostic at ASDEX Upgrade,"
- [4] D. Wendler, R. Dux, R. Fischer, M. Griener, E. Wolfrum, G. Birkenmeier, U. Stroth, and the ASDEX Upgrade Team, "Collisional radiative model for the evaluation of the thermal helium beam diagnostic at ASDEX Upgrade.," *Plasma Phys. Control. Fusion* **64** (2022)



## Fully relativistic calculation of cross sections and their application in identifying suitable emission lines for the diagnostics of non-equilibrium plasmas

**Indhu Suresh<sup>1</sup>, Priti<sup>2</sup>, R Srivastava<sup>3</sup>, and R K Gangwar<sup>1</sup>**

<sup>1</sup>*Department of Physics & CAMOST, Indian Institute of Technology Tirupati, Tirupati, 517619, India*

<sup>2</sup>*National Institute for Fusion Science, Gifu, 506-5292, Japan*

<sup>3</sup>*Department of Physics, Indian Institute of Technology Roorkee, Roorkee, 247667, India*

Accurate plasma diagnostics are essential for comprehending their physics and practical applications in various fields, including astrophysics, fusion research, semiconductor manufacturing, and so on. Spectroscopy-based diagnostic techniques serve as potent tools for characterizing various types of plasmas, including those found in extreme conditions such as fusion plasmas. Optical emission spectroscopy (OES) is the commonly employed spectroscopic technique due to its non-invasive nature and robustness. Yet, achieving accurate characterization necessitates the integration of OES measurements with appropriate plasma population kinetic models. However, it's important to note that most of the plasmas we deal with deviates significantly from complete/local thermodynamic equilibrium and hence the equilibrium models are no longer applicable. Collisional Radiative (CR) model is a prominent population kinetic model extensively utilized for the diagnostics of non-equilibrium plasmas. It helps in extracting plasma parameters, tracking their spatio-temporal evolution, and in identifying emission lines suitable to probe the qualitative behaviour of plasma parameters in real-time monitoring. The mechanisms that populate and depopulate the emitting states constitute a coupling between the collisional and radiative processes inside the plasma. The excitation mechanisms that result in plasma emission are dominated by the inelastic collision of plasma electrons with atoms, molecules, and ions. Hence, it is crucial to calculate the cross sections for electron impact excitation processes accurately.

In light of this we have performed the calculations of fine structure resolved excitation cross sections using the relativistic distorted wave approximation theory with the aid of multi configurational Dirac Fock wavefunctions as the target states *i.e.*, Mo, Sn, Ga and Al, for a wide range of incident electron energies (threshold to 500 eV) [1, 2]. The accuracy of the wavefunctions employed in our calculations is validated by comparing excitation energies, oscillator strengths, and transition probabilities with previously reported results. The calculated cross sections are compared with available measurements and calculations to ensure their consistency. Furthermore, the calculated cross sections are successfully implemented in the CR model for the diagnostics of various non-equilibrium plasmas of Mo, Sn, Ga and Al [1, 2]. In addition to this, suitable line ratios for the determination of the plasma parameters are also proposed. The detailed results, along with methodology and discussions, will be presented at the school.

[1] Indhu Suresh et al, Plasma Sources Sci. Technol. **32**, 075006 (2023).

[2] Indhu Suresh et al, Plasma Sources Sci. Technol. **31**, 095016 (2022).

## Hyperfine-induced effects on the linear polarization of the magnetic-quadrupole lines of spin-1/2 Be-like ions excited by electron impact

Ziqiang Tian<sup>1</sup>, Zhiming Tang<sup>1</sup>, Yi Li<sup>2</sup>, Yang Yang<sup>1,\*</sup>, Zhongwen Wu<sup>2,3,4</sup>, and Yaming Zou<sup>1</sup>

<sup>1</sup>Shanghai EBIT Laboratory, Key Laboratory of Nuclear Physics and Ion-Beam Application (MOE), Institute of Modern Physics, Fudan University, Shanghai 200433, China

<sup>2</sup>Key Laboratory of Atomic and Molecular Physics and Functional Materials of Gansu Province, College of Physics and Electronic Engineering, Northwest Normal University, Lanzhou, 730070, China

<sup>3</sup>Helmholtz-Institut Jena, Fröbelstieg 3, D-07743 Jena, Germany

<sup>4</sup>GSI Helmholtzzentrum für Schwerionenforschung GmbH, Planckstrasse 1, D-64291 Darmstadt, Germany

The polarization of X-rays has been employed as an effective tool to study various physical effects including the hyperfine interaction. However, most studies mainly focused on the lines emitted from the strong  $2p \rightarrow 1s$  transition. In fact, the  $2p \rightarrow 2s$  transition is more weaker than the  $2p \rightarrow 1s$  transition, and thus its hyperfine-induced effects are more pronounced. For this purpose, we have studied the linear polarization of the magnetic-quadrupole (M2) lines  $1s^2 2s 2p_{3/2} \ ^3P_2 \rightarrow 1s^2 2s^2 \ ^1S_0$  and  $1s 2s^2 2p_{3/2} \ ^3P_2 \rightarrow 1s^2 2s^2 \ ^1S_0$  following the electron-impact excitation of Be-like ions with nuclear spin  $I=1/2$  by using the density-matrix theory and the relativistic distorted-wave theory [1]. To explore the effects of the hyperfine interaction, detailed calculations are performed for the polarization of the M2 lines emitted from  $^A\text{Xe}^{50+}$  ( $A = 125, 127, \text{ and } 129$ ) and  $^A\text{Tl}^{77+}$  ( $A = 187, 205, \text{ and } 207$ ) ions with different nuclear magnetic dipole moments  $\mu_I$  at a series of impact electron energies. It is shown that the hyperfine interaction strongly lowers the polarization of the  $1s^2 2s 2p_{3/2} \ ^3P_2 \rightarrow ^1S_0$  line at all considered impact energies, while its effects behave less and less prominent with increasing impact energy for the  $1s 2s^2 2p_{3/2} \ ^3P_2 \rightarrow ^1S_0$  line. In addition, we also find that the polarization of the  $1s^2 2s 2p_{3/2} \ ^3P_2 \rightarrow ^1S_0$  line is much more sensitive to  $\mu_I$  than that of the  $1s 2s^2 2p_{3/2} \ ^3P_2 \rightarrow ^1S_0$  line. In particular, for the  $1s^2 2s 2p_{3/2} \ ^3P_2 \rightarrow ^1S_0$  line of spin-1/2  $\text{Xe}^{50+}$  ions, the differences in the polarization among the isotopes are significant. These findings indicate that precise polarization measurements of M2 lines of Be-like ions are expected to be used to explore the hyperfine interaction and even the nuclear magnetic dipole moment of nonzero-spin isotopes.

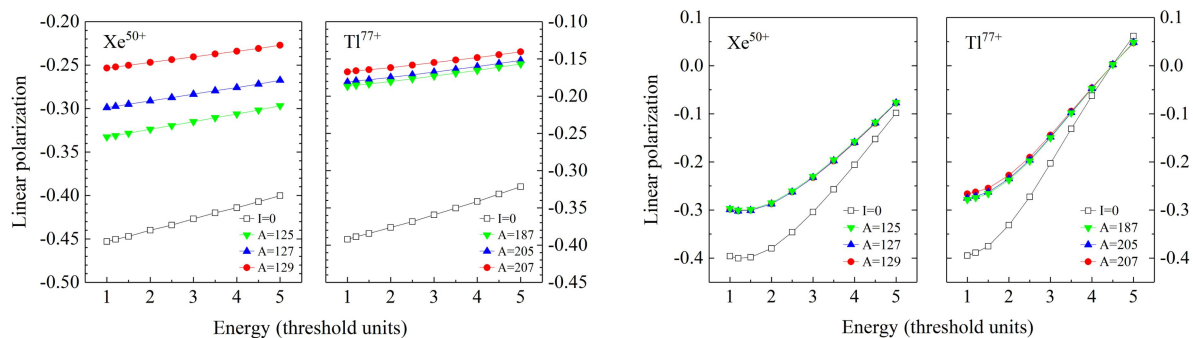


Figure 1. Linear polarization of the M2 lines  $1s^2 2s 2p_{3/2} \ ^3P_2 \rightarrow ^1S_0$  (left pane) and  $1s 2s^2 2p_{3/2} \ ^3P_2 \rightarrow ^1S_0$  (right) emitted from zero-spin Be-like ions as well as spin-1/2 Be-like  $^A\text{Xe}^{50+}$  ( $A = 125, 127, \text{ and } 129$ ) and  $^A\text{Tl}^{77+}$  ( $A = 187, 205, \text{ and } 207$ ) ions at an angle of  $\theta = 90^\circ$  relative to the quantization axis as functions of impact electron energy in units of their respective excitation threshold.

[1] Z. Q. Tian, Z. M. Tang, Y. Li, Y. Yang, Z. W. Wu, Y. M. Zou, *J. Quant. Spectrosc. Radiat. Transfer* 311, 108775 (2023).

## Tomographic reconstructions of the 2D emission distributions of impurity with EAST visible tangential wide-angle viewing systems

**B. G. Wang<sup>1</sup>, R. Ding<sup>1</sup>, D. H. Zhu<sup>1</sup>, R. Yan<sup>1</sup>, B. F. Gao<sup>1</sup>, J. H. Yang<sup>1</sup>, C. N. Xuan<sup>1,2</sup>, Y. Wang<sup>1,2</sup>, and J. L. Chen<sup>1</sup>**

<sup>1</sup> *Institute of Plasma Physics, Hefei Institutes of Physical Science Chinese Academy of Sciences, Hefei 230031, China*

<sup>2</sup> *University of Science and Technology of China, Hefei 230026, China*

The amount and spatial distribution of impurity radiation in the divertor of a tokamak is of fundamental importance for the behaviours of power exhaust, detachment and erosion/re-deposition properties [1]. The visible tangential wide-angle viewing systems for its high spatial, temporal resolution and data visualization, is widely used in fusion devices. Tomographic reconstructions of tangential camera views are an established method for resolving the 2D distribution of divertor emission in various tokamak devices [2]. Four integrated infrared and visible tangential wide-angle viewing systems (WAVS) and one multi-band wide-angle high-speed viewing systems (MWHVS) have been mounted in Experimental Advanced Superconducting Tokamak (EAST).

Plasma emission of impurities is measured with MWHVS equipped with interference filter of bandwidth centred on the CIII (400.88 nm) emission line during the CD4 seeding from the lower divertor. The inverse problem includes: calibration of the detailed camera viewing geometry and the tomographic inversion. A Zhang's calibration algorithm [3] is utilized to calibrate the intrinsic, extrinsic and distortion parameters of MWHVS using checkboard with the geometric dimensions of  $(12 \times 9) \times 0.06\text{m}$ . With the help of the transformation between the EAST real world coordinate and the camera coordinate, The pixel and camera positions in EAST coordinate are calculated. By modeling the 2D camera image pixels as line of sight integrals through an axisymmetric discrete grid, the sparse response matrix is calculated. To obtain the poloidal plasma line emission distributions, the Algebraic Reconstruction Technique (ART) is used to solve the sparse matrix-vector linear system. The tomography reliability has been tested with a known emission function where the error is also discussed. The typical tomography results have been analyzed for the EAST shot (#117765) with the CD4 seeding from the lower divertor to achieve the detachment phase. The peak intensity of the CIII migrates from the lower outer strike point to the LCFS near the high field side during the detachment. And also, the temperature of the lower divertor measure by the IR camera is decreased.

[1] A. Huber, et al., Journal of Nuclear Materials 313-316 (2003) 925-930.

[2] W. H. Meyer, et al., Review of Scientific Instruments 89, 10K110 (2018).

[3] Z. Y. Zhang. IEEE Transactions on Pattern Analysis & Machine Intelligence, 2000.

## Comparative modeling of neon and tungsten impurity transport in the boundary plasma of EAST with normal and extended grid to the first wall

Hui Wang<sup>1</sup>, Guoliang Xu<sup>1</sup>, Rui Ding<sup>1</sup>, Hang Si<sup>1</sup>, Guozhang Jia<sup>1</sup>, Hai Xie<sup>1</sup>, Junling Chen<sup>1</sup>

*1 Institute of Plasma Physics, Hefei Institutes of Physical Science, Chinese Academy of Sciences, Hefei 230031, China*

The impurity leakage mechanisms of seeded neon and eroded W in the boundary plasma of EAST are revealed by modeling using the coupled SOLPS-DIVIMP codes with full drift effects included. The Ne distribution derived from the impurity tracing Monte Carlo DIVIMP simulation using the background plasma from the SOLPS-ITER simulation agrees well with the Ne transport by fluid SOLPS-ITER simulations, which validates the implemented drift effects. Then the leakage processes of both Ne and W under various dissipative divertor conditions are investigated by the DIVIMP code. An increase of both Ne and W concentration in the core plasma is observed before the onset of divertor detachment when increasing the Ne injection rate. Meanwhile, Ne shows a larger leakage ability than that of W under both attached and detached divertor conditions due to the more pronounced impact of drifts on Ne transport. Modeling results reveal that under the favorable  $B_t$  direction,  $E \times B$  drifts can drive impurities from the outer divertor region to the inner divertor region, and increase the impurity leakage from the inner divertor region where the poloidal  $E \times B$  drift points upstream. To study W source and transport from the first wall, the simulation grid is extended to the first wall based on a low single null divertor configuration. The OSM-EIRENE is used to generate the background plasma and the W erosion and transport is then calculated using the DIVIMP code with a full W wall condition. Comparative analysis between results from the normal and extended grids shows significant changes in the W source and leakage paths. Under the favorable  $B_t$  direction, the  $E \times B$  drifts lead to an enrichment of Ne in the inner divertor region and facilitate the onset of detachment. However, a notable W source comes from the first wall of the high-field side (HFS) adjacent to the divertor due to the high Ne impinging flux, even if the divertor is detached. Since the poloidal  $E \times B$  drift facilitates the W leakage from the HFS, the W core concentration of the extended grid is much higher than that of the standard grid. Consequently, the inclusion of an extended grid for modeling is important to for understanding W source and leakage with full W wall tokamaks.

## Deuterium retention analysis in pre-damaged tungsten using laser-induced breakdown spectroscopy

Erik Wüst<sup>1,2</sup>, Christoph Kawan<sup>1,2</sup>, Sebastijan Brezinsek<sup>1,2</sup>, and Thomas Schwarz-Selinger<sup>3</sup>

<sup>1</sup>*Forschungszentrum Jülich GmbH, Institut für Energie und Klimaforschung - Plasmaphysik, Partner of the Trilateral Euregio Cluster (TEC), 52425 Jülich, Germany*

<sup>2</sup>*Faculty of Mathematics and Natural Sciences, Heinrich Heine University Düsseldorf, 40225 Düsseldorf, Germany*

<sup>3</sup>*Max-Planck-Institut für Plasmaphysik, D-85748 Garching, Germany*

Energetic neutrons are a product of the DT-fusion reaction and can induce material damage in Plasma-Facing Components (PFCs) in future nuclear fusion reactors. The damage increases with time and causes enhanced fuel, tritium (T) and deuterium (D), retention in tungsten (W) PFCs, which imposes issues for safety and closure of the T cycle in the fusion plant. Laser-Induced Breakdown Spectroscopy (LIBS) is a potential in-situ technique to monitor tritium inventory in W PFCs. LIBS on pre-damaged W (W ions, 10.8 MeV, 0.23 dpa) with D contents of 0.1-1% owing to D plasma exposure in PlaQ and subsequent outgasing, was carried out to measure the depth-resolved fuel content in a laboratory set-up. LIBS was done using an Nd:YAG laser (35 ps, 355 nm, 20 mJ), ablating 15 nm per laser pulse. D was detected up to a depth of  $1.3\mu\text{m}$  by observing Balmer  $\alpha$  line from the laser-induced plasma plume. The depth profile and total amount was compared with nuclear reaction analysis (NRA) and showed good agreement. Deviations can only be observed for the first ablation cycle near the surface.

## High energy density material produced by heavy ion beam drive

Xiaoxia Wu<sup>1</sup>, Lingrui Liao<sup>2</sup>, Wei kang<sup>2</sup>, Rui Cheng<sup>1,3</sup>, Jie Yang<sup>1,3</sup>, and Xinwen Ma<sup>1,3</sup>

<sup>1</sup> Institute of Modern Physics, Chinese Academy of Sciences, Lanzhou 730000, China

<sup>2</sup> Peking University, Beijing 100871, China

<sup>3</sup> University of Chinese Academy of Sciences, Beijing 100049, China

The purpose of this report is to demonstrate the potential for high energy density physics (HEDP) research on the HIAF facility. The study of HEDP involves a wide range of fundamental and applied physics. For example, astrophysics, planetary science, geophysics, plasma physics, hydrodynamics, radiation hydrodynamics, magnetohydrodynamics, materials science, condensed matter physics, the interaction of intense radiation with matter, and atomic and molecular physics and so on. In addition, the field has great potential for many lucrative industrial applications. The study of the fundamental properties of HED matter is therefore not only of great scientific importance, but also of great technological significance[1, 2].

The study of high energy density physics based on heavy ion beams has unique advantages. The Aardvark programme developed based on the hydrodynamic equations. The equation of state for warm dense matter is calculated from first principles. The Aardvark program was used to simulate the beam-target coupling experiment, which provides guidance for the HIAF facility to carry out high energy density physics experiments in the future. The thermodynamic and hydrodynamic response of a solid lead cylindrical target was investigated by one-dimensional hydrodynamic simulations. One side of the target is irradiated by a uranium ion beam such that the beam axis coincides with the cylindrical axis. The range of the ions is much larger than the length of the target, so that the Bragg peak is located outside the target and uniform energy deposition occurs along the beam trajectory. A radial outward shock wave is produced. The results are shown in Figure 1.

Simulation parameters consistent with the HIAF facility are selected. To verify the stability and robustness of the procedure, we conducted extensive simulations, systematically altering the beam and target parameters. Simulation results indicate that the ion beam from the HIAF facility will have sufficient power for the production of high energy density materials in a laboratory environment. These studies will enhance our comprehension of the creation, development and essential characteristics of high-energy-density matter. They will give theoretical backing and practical direction for possible implementations in domains such as defence, energy and astrophysics.

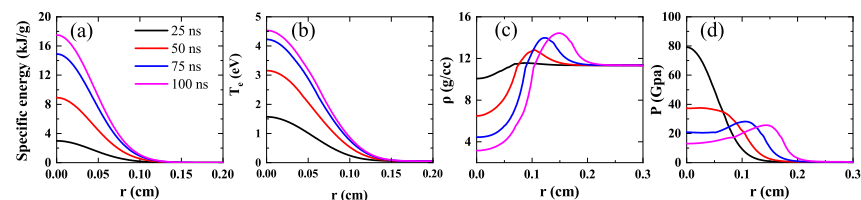


Figure 1: Evolution of deposited energy, electron temperature, density and pressure along the radial direction at the ion beam intensity of  $10^9$  particle per pulse

[1] Tahir, N. A. et al., Phys. Rev. Lett. **95**, 035001 (2005).

[2] Tahir, N. A. et al., ApJS. **238**, 27 (2018).

**Joint ICTP-IAEA School on Data for Modelling Atomic and Molecular Processes in Plasmas I (smr 3924)**

**Charge exchange recombination spectroscopy of Ta<sup>9+</sup> for application to DIII-D and ITER neutral hydrogen beam diagnostics**

**P. N. Yaron**<sup>1</sup>

*Flinders University, Institute for NanoScale Science and Technology  
Bedford Park, South Australia*

Tantalum has shown promise as a potential plasma facing material, due to its similar physical and chemical properties to Tungsten with the added ability to remove neutral Hydrogen atoms in the plasma edge. Reducing the number of charge exchange events reduces net energy losses in the plasma, potentially improving performance of fusion for energy devices. Cold spray deposited coatings of Tantalum on 316L steel have been developed at the University of Wisconsin, Madison. Initial experimentation has shown ‘excellent structural stability’ [1].

This work seeks to validate reduced charge exchange events using theoretical modelling of charge exchange recombination spectroscopy (CXRS). The model will be based on interactions of neutral beams at DIII-D [2] where further *in-situ* experimentation will most likely be performed using the Divertor Material Evaluation System (DiMES) [3]. The model will be extended to ITER diagnostic and heating beam conditions. A CR model will developed closely following the methodologies outlined previously by Ralchenko et. al. [4].

[1] M. Ialovega et al. Phys. Scr. **98**, 115611 (2023).

[2] ‘DIII-D National Fusion Program Five-Year Plan 2019 – 2024’ GA Report-A28765 (2018).

[3] D.L. Rudakov Fusion Engineering and Design **124**, 196–201 (2017).

[4] Dipti et al. Plasma Phys. Control. Fusion **63** 115010 (2021).